Article

Making Historical Gyroscopes Alive – 2D and 3D Preservations by Sensor Fusion and Open Data Access

Dieter Fritsch[1,*], Jörg F. Wagner[2], Beate Ceranski[3], Sven Simon[4], Maria Niklaus[3], Kun Zhan[2] and Gasim Mammadov[4]

[1] Institute for Photogrammetry, University of Stuttgart; dieter.fritsch@ifp.uni-stuttgart.de
[2] Chair of Adaptive Structures in Aerospace Engineering, University of Stuttgart; jfw@pas.uni-stuttgart.de
[3] Institute of History, University of Stuttgart; beate.ceranski@hi.uni-stuttgart.de
[4] Institute of Parallel and Distributed Systems, University of Stuttgart; Sven.Simon@ipvs.uni-stuttgart.de

* Correspondence: dieter.fritsch@ifp.uni-stuttgart.de; Tel.: +49-151 15286238

Abstract: The preservation of cultural heritage assets of all kind is an important task for modern civilizations. This also includes tools and instruments that have been used in the previous decades and centuries. Along with the industrial revolution 200 years ago, mechanical and electrical technologies emerged, together with optical instruments. In the meantime, not only museums are showcasing these developments, but also companies, universities, and private institutions.

Gyroscopes are fascinating instruments with a history of about 200 years. When J.G.F. Bohnenberger presented his machine to his students in 1810 at the University of Tuebingen, Germany, nobody could have foreseen that this fascinating development would be used for complex orientation and positioning. At the University of Stuttgart, Germany, a collection of 160 exhibits is available and in transition for a sustainable future. Here, the systems are digitized in 2D, 2.5D and 3D and are made available for a world-wide community using OpenAccess platforms. The technologies being used are Computed Tomography, Computer Vision, Endoscopy and Photogrammetry. The workflows for combining voxel representations and colored point clouds are described, to create Digital Twins of the tangible assets. Advantages and disadvantages are discussed und work for near future is outlined in this new and challenging field of Tech Heritage digitization.

Keywords: History of technology, Computer Vision, Photogrammetry, Endoscopy, Computed Tomography, Convolutional Neural Networks, Structure-from-Motion, Dense Image Matching, Data Fusion, Sensor Fusion, Digital Twin, Navigation Instruments, Inertial Sensors.

1. Introduction

The preservation of cultural heritage assets - tangible and intangible - is an important task of modern civilizations. This provides identity, ensures the understanding of the past, the identification with traditions and customs, and allows for accessing existing, destroyed or lost heritage objects.

Tangible assets of cultural heritage include also technical instruments and artifacts – we call it Tech Heritage (TH). If these assets are historically researched and didactically processed, they allow for insights into developments and objects that have fundamentally shaped our civilization. Without professional processing, however, these assets remain silent; especially when they are technically complex and significantly encapsulated.

There are several methods and technologies for 3D preservations of outdoors cultural heritage (CH) objects available and well-described in literature – a most recent review is given by [1]. These are differentiated in active and passive sensing. Active sensors collect mostly range-based 3D data,

Preprints (www.preprints.org) | NOT PEER-REVIEWED | Posted: 8 December 2020 doi:10.20944/preprints202012.0205.v1

by invasive direct measurements of mechanical systems or operating optical systems using triangulations, Time-of-Flight (ToF) or interferometry. Therefore, active sensing technologies used so far in outdoors CH applications seem to be less suitable for 3D preservations of TH objects.

This scenario completely changes, when evaluating the methods and technologies of medical imaging. In medicine, a variety of methods for generating 3D volume data have been developed and are now widely used in medical applications to visualize the internal structures of the human organism, such as magnetic resonance imaging (MRI), positron emission tomography (PET) but to an even greater extent X-ray based computed tomography (CT). CT is nowadays used for a variety of sciences and applications beyond the medical field, such as material sciences, physics, biology, mechanical engineering or technical applications to non-destructively determine three-dimensional models for the internal structures of objects. For example, several studies in non-medical fields have been carried out by the authors of this paper and others using computed tomography: Measurement of the properties of electrical structures [2], application of dimensional metrology [3, 4, 5, 6], and contactless and non-destructive three-dimensional digitization and conservation of cultural assets in the context of digital heritage [7, 8, 9, 10]. These non-medical applications are drivers for computed tomography systems with ever higher spatial resolution from the micrometer to the nanometer range as well as for X-ray-based computed tomography systems with ever higher photon energies in order to irradiate materials that absorb much more strongly than tissues, such as metals and greater radiolucent material thicknesses. In summary, using medical technologies, such as CT, extend existing methods of active sensing to collect 3D data inside a TH object.

Passive sensing is image-based using the natural light or enhanced lightning conditions. Based on the well-known methods and technologies for aligning and matching overlapping image blocks, as offered by geometric Computer Vision (CV) and photogrammetry, we also integrate endoscopy to collect overlapping images inside of TH objects (see Figure 1). The steps for all three fields are more or less identical: Firstly, we collect images with calibrated photo cameras and endoscopes. Secondly, the images are aligned by Structure-from-Motion (SfM) or Bundle Block adjustment. Thirdly we accomplish dense image matching (DIM) to get colored dense point clouds in 2,5D. And, fourthly, the 2,5D colored point clouds are filtered and meshed to obtain "watertight" 3D models.

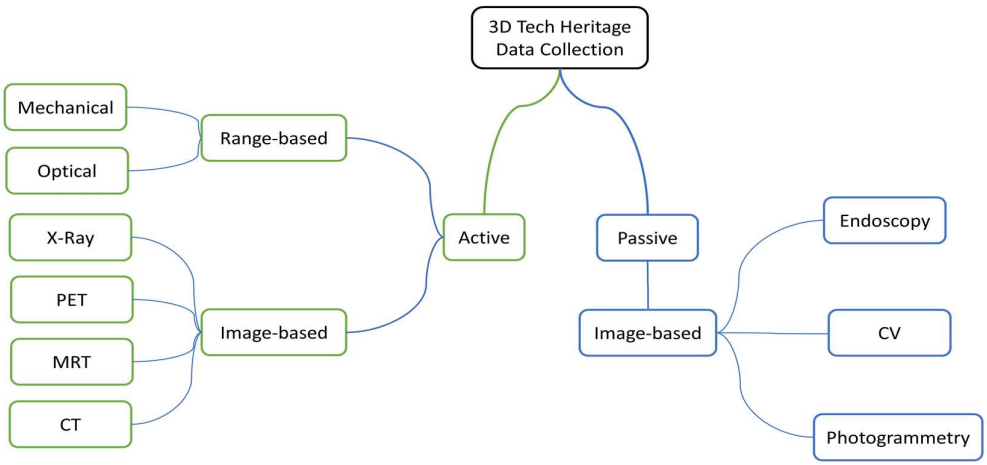

Figure 1. Taxonomy for 3D Tech Heritage Data Collections.

The last twenty years have seen important milestones pass in the processing stereo and multi-view stereo data, likewise in geometric CV and photogrammetry. The relation between photogrammetry and CV [11] has been considerably improved. It was proven, that the projective equations of CV are identical with the collinearity equations of photogrammetry and therefore methods can be exchanged between them. Automatic image feature detection was boosted by [12] [13] to get tie points for SfM (geometric CV) and bundle block adjustment (photogrammetry). In 2000 [14] published the 1st edition

Preprints (www.preprints.org) | NOT PEER-REVIEWED | Posted: 8 December 2020 doi:10.20944/preprints202012.0205.v1

of a comprehensive collection of multiple view methods in CV. With [15] Semi-global Matching (SGM) was introduced leading to superb quality and resolution of point clouds. [16] demonstrated a accurate, dense and stereo reconstruction using SGM. A refinement of SGM is tube-based SGM or tSGM and led to the development of SURE [17] [18], a software for Dense Image Matching (DIM) for airborne [19], close range imagery [20] and most recently for space-borne high resolution optical imagery [21]. Another refinement of the SGM algorithm is given by [22].

Preserving Tech Heritage in 3D by a combination of CT, CV, endoscopy and photogrammetry is a new and fascinating field allowing for many options, in historical research, education, and AR/VR visualizations. At a first stage, a 3D model of an instrument – inside and outside - by a meshed and watertight point cloud is offered, which can be shared in OpenAccess (OA) with a wordwide community. Thus, any intersections can be generated, using Open Source (OS) software, e.g. CloudCompare, MeshLab, the Point Cloud Library, Pointools etc.. A next level is the decomposition into Computational Solid Geometry (CSG) features, e.g vectorial elements, which finally represent all parts in a lego-like fashion. Another benefit of a CSG description is data compression and semantic labeling. Up to now, CSG modeling is accomplished with satisfying output only through very time-consuming manual work. In future, the methods of Machine Learning and Deep Learning might help to automate this decomposition. Therefore, with this research we are entering largely unexplored territory that holds the promise of many exciting developments in the years to come.

The structure of this article is as follows: Section 2 describes the novum of this work to combine 2.5D models of geometric Computer Vision with 3D voxels of Computed Tomography. Point clouds are normally fused and co-registered using the ICP algorithm with no explicit information about the in-depth geometric quality. We define a spatial similarity transformation embedded in a Gauss-Helmert model to get finally variances of the unit weight and standard deviations of the fused data sets. Section 3 describes the University of Stuttgart's gyroscopes collection, which was launched in the 1960s and contains about 160 objects. To sustain these TH assets the Gyrolog project started 2017 with the mission to generate digital twins using Computed Tomography (CT), geometric Computer Vision (CV) and photogrammetry. In addition, the potential of endoscopy was to be explored. Section 4 deals with 2D photography and post-processing for easy object documentation and digital archiving. The details to collect 3D CT scans with denoising characteristics and 2.5D colored point clouds of CV/photogrammetry and endoscopy to finally get a 3D digital twin are outlined in Section 5. The basic workflows and experimental results are presented. Section 6 contains exemplarily the 3D reconstructions of three different gyroscopes including some history research: The Machine of Bohnenberger (1810), which is regarded as the very first gyroscope, then a directional gyroscope for aircrafts in World War 2 (1940s) and a gyroscope embedded in the inertial platform of the Lockheed F104G Starfighter (1960s). Moreover, further two examples demonstrate our capability to create 3D digital twins of the Stuttgart gyroscope collection. Thereafter the curation and sustainability in OA environments are outlined in Section 7. Finally, the conclusions and an outlook for future work complete this article.

2. Merging 2.5D and 3D Data and Texturing – Making 3D Models Alive

In order to generate digital twins of Tech Heritage objects, such as the very first gyroscope invented by J.G.F. Bohnenberger in 1810 (see Figure 2), we decided to go for a combination of CT, Endoscopy and CV/Photogrammetry. As will be shown later, sensor fusion for this combination is only possible with endoscopy and CV/photogrammetry, as both generate optical image blocks to be processed by SfM and DIM in one processing step. This finally leads to consistent alignments and co-registered colored 2.5D point clouds.

The co-registration of CV/photogrammetry point clouds with 3D CT scans is only possible by data fusion using registration algorithms, such as the Rigid Body transform or a spatial similarity transformation. A classical approach is the Iterative Closest Point (ICP) algorithm, as given by [23] and implemented in Open Source point cloud libraries, such as CloudCompare, MeshLab, PCL and Open3D. But its disadvantage is the missing in-depth quality measure for the registration. Thus, we define a 7 parameter spatial similarity transformation embedded in an adjustment model, for not

Preprints (www.preprints.org) | NOT PEER-REVIEWED | Posted: 8 December 2020 doi:10.20944/preprints202012.0205.v1

only to co-register the 3D CT scans with the 2.5D point clouds of CV/photogrammetry, but also to get quality measures for the registration in form of unit weight variances and standard deviations.

(a) (b) (c)

Figure 2. The very first gyroscope of 1810 – the Machine of Bohnenberger, Tuebingen, Germany. (a) Original drawing; (b) Photo; (c) 3D digital twin by CV/photogrammetry.

Starting with the 7 parameter transformation with at least 3 control points, we get

$$\boldsymbol{X} = \boldsymbol{X}_o + \mu \boldsymbol{R}\boldsymbol{x} \quad (1)$$

with $\boldsymbol{X}$ the $(3x1)_u$ vector of the target coordinates of u control points, $\boldsymbol{X}_o$ the $(3x1)_u$ vector of the 3 translation parameters (X_o, Y_o, Z_o), μ is the scale, $\boldsymbol{R}$ the $(3x3)_u$ rotation matrix depending on the unknown rotation angles α, β, γ and $\boldsymbol{x}$ the $(3x1)_u$ vector of the local u control point coordinates. This non-linear transformation is linearized considering only differential changes in the three translations, three rotations and one scale, and therefore replacing (1) by

$$\boldsymbol{dx} = \boldsymbol{S}\,\boldsymbol{dt} \quad (2)$$

$\boldsymbol{S}$ is the $(3x7)_u$ similarity transformation matrix resulting from the linearization process of (1), and

$$\boldsymbol{dt'} = [dx_o, dy_o, dz_o, d\alpha, d\beta, d\gamma, d\mu] \quad (3)$$

representing the seven unknown registration parameters. In order to estimate the precision of the registration, a least-squares Gauss-Helmert model [24] must be solved, for $u \geq 3$ and $\boldsymbol{B} := \boldsymbol{S}$ leading to

$$1^{st} \text{ order: } \boldsymbol{A}\boldsymbol{v} + \boldsymbol{B}\boldsymbol{x} + \boldsymbol{w} = \boldsymbol{0}, \quad \text{and} \quad 2^{nd} \text{ order: } D(\boldsymbol{v}) = \sigma^2 \boldsymbol{P}^{-1} \quad (4)$$

Solving (4) with respect to $\boldsymbol{v}$, $\boldsymbol{x}$ and the Lagrangian $\boldsymbol{\lambda}$ we use Gaussian error propagation for getting the desired dispersion matrices. With $D(\boldsymbol{w}) = \sigma^2 \boldsymbol{A}\boldsymbol{P}^{-1}\boldsymbol{A}'$ the precision of the registration parameters is propagated to

$$D(\boldsymbol{x}) = \sigma^2 [\boldsymbol{B}'(\boldsymbol{A}\boldsymbol{P}^{-1}\boldsymbol{A}')^{-1}\boldsymbol{B}]^{-1} \quad (5)$$

$D(\boldsymbol{x})$ contains the variances and covariances along its main diagonal and the off-diagonals, which can be used to propagate any precision of the individual in-situ data collection method and finally assess the quality of the registration.

Let be $V(O)$ the set of m voxels of a 3D CT scan and $P(O)$ the set of n points describing the object hull (2.5D) of CV/photogrammetry, first of all the Ground Sampling Distance (GSD) or Object Sampling Distance (OSD) of the CT scan must be down-sampled being similar to the CV/photogrammetry OSD (see Figure 3). Then the CT voxels are to be transformed to point clouds, i.e. $V(O) \rightarrow VP(O)$ representing a similar data structure of $P(O)$. The next step is to choose $u > 3$ homologue points for the co-registration of $VP(O)$ with $P(O)$.

Preprints (www.preprints.org) | NOT PEER-REVIEWED | Posted: 8 December 2020 doi:10.20944/preprints202012.0205.v1

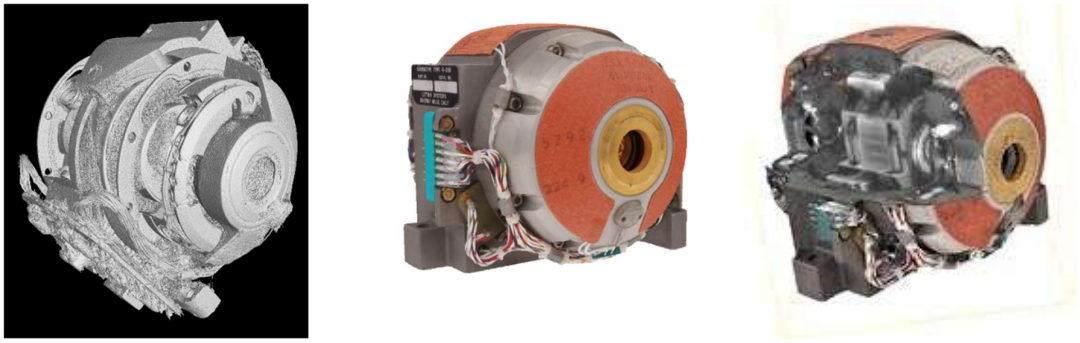

(a) (b) (c)

Figure 3. Example for co-registration of CT Scans with CV/photogrammetry point clouds – the 3D digital twin of the Gyro200 (see Section 6.3): (a) Iso-surface of a denoised Filtered Back Projection (FBP) CT scan; (b) convex hull generated by CV/photogrammetry; (c) Cross-section of the integrated CT and CV/photogrammetry 3D reconstruction.

The OSD of CV/photogrammetry for our applications is around 0.05 – 0.09mm, and the CT scan OSD is about 0.06mm. Thus the OSDs are similar but CT provides larger data volumes. For the example of Figure 3 the CT scan of original resolution is about 86GB and the CV/photogrammetry point cloud is about 440MB. The down-sampling of CT by a factor of 4 reduces the data volume to 1.34GB and also the noise and artifacts. After an initial application of the ICP algorithm using OS libraries we choose u=4 and u=10 mutual corners of the merged point clouds and get finally improved registration results with the following quality measures for precision: For u=4 the estimated variance of unit weight σ=1.38 and σ_{CT}=0.10mm, σ_{CV}=0.08mm, and for u=10 we get σ=1.07, σ_{CT}=0,08mm and σ_{CV}=0,06mm. The more control points that are used, the better the reliability of the precision can be estimated. These figures demonstrate that CV/photogrammetry 2.5D point clouds are slightly more precise than down-sampled CT 3D volume data and efforts are to made to reduce noise and artifacts in CT scans (see section 5.1) to come to the same level of precision.

3. The University of Stuttgart's Gyroscopes Collection – the Gyrolog Project

Based on J.G.F. Bohnenberger's 1810 invention of the gimbal mounted gyro, also called the Machine of Bohnenberger, and the work continued by J.B.L. Foucault to prove the Earth's rotation, the theory of the gyroscope became a supreme discipline of physics, during the 19th century [25, 26]. The first technical applications followed at the beginning of the 20th century. Scientists like F. Klein, A. Sommerfeld and M. Schuler at the University of Goettingen and R. Grammel at the Technical University of Stuttgart as well as entrepreneurs like H. Anschuetz-Kaempfe, Kiel, and W. v. Siemens, Berlin, made Germany a world leader in gyroscopes for flight and ship control, both scientifically and industrially. After World War 2, K. Magnus, M. Schuler's student and R. Grammel's successor in Stuttgart, as well as the companies Anschuetz (Kiel), Bodenseewerk (Ueberlingen), C. Plath (Hamburg), Litef (Freiburg) and Teldix (Heidelberg) resumed this tradition [27].

Understanding the movement of the gimbal-mounted gyro and its derivatives is considered to be particularly challenging, both physically and mathematically [28]. To illustrate the teaching and research of K. Magnus, he and his assistants H. Sorg and J. Steinwand started in the 1960s to assemble a collection of gyroscopes at the Institute of Mechanics of the Faculty of Mechanical Engineering, University of Stuttgart. In 2005 the responsibility for the collection passed on to J.F. Wagner, Faculty of Aerospace Engineering and Geodesy at this University.

In addition to illustrating how gyroscopes and inertial navigation systems work, the collection also reflects the historical development of these instruments. It is also supplemented by other devices for guiding aircrafts such as compasses, altimeters and variometers. It contains approx. 160 objects and

Preprints (www.preprints.org) | NOT PEER-REVIEWED | Posted: 8 December 2020 doi:10.20944/preprints202012.0205.v1

includes most of the known types of gyro instruments for flight, land vehicle and ship navigation (gyro compass, directional gyro, gyro horizon, P and I rate gyros, etc.) as well as various types of accelerometers. There are also complete inertial platforms. Components of the devices such as rotors, slip rings and rotary encoders as well as rotary tables for testing inertial sensors are also available. Many exhibits were taken from decommissioned aircrafts and ships. Some of them have been cut open or partly dismantled, and some are still operational. Their age is mostly between 40 and 70 years. This records the development of gyroscopic instruments, especially from the work of H. Anschuetz-Kaempfe, Kiel, and E. Sperry, New York, up to the 1970s. The collection is unique for the higher education sector, at least in Germany, and is also complementary to other important collections of this type not only in Germany but worldwide. An excerpt of some objects is on display in Figure 4.

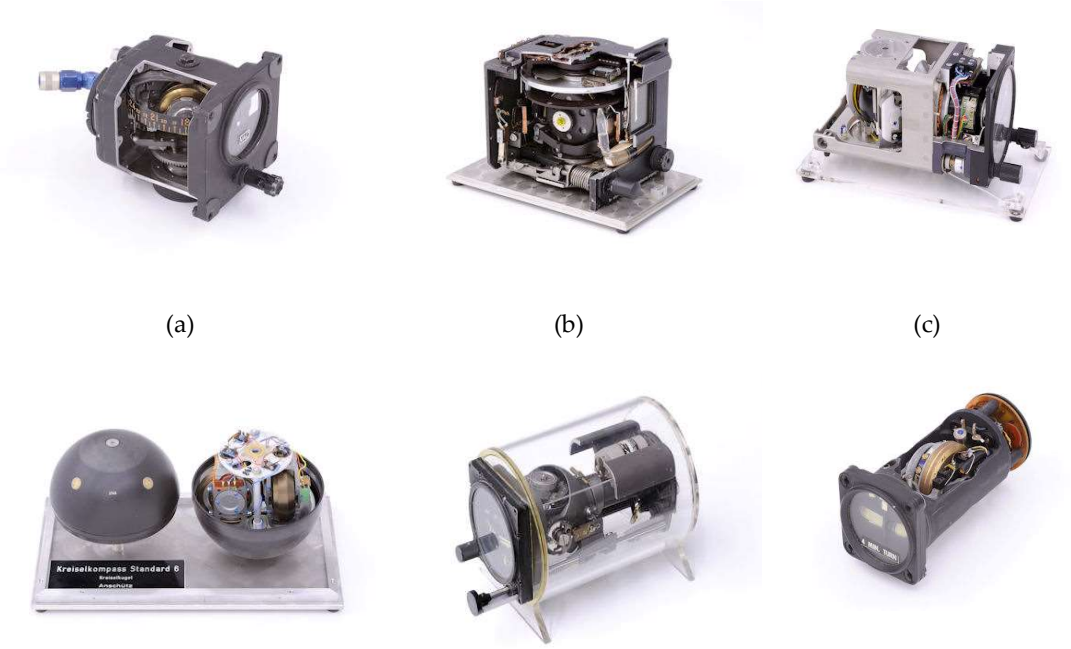

(a) (b) (c)

(d) (e) (f)

Figure 4. Excerpt of the University of Stuttgart's gyroscope collection (Photos: B. Miklautsch, Photography Lab, University of Stuttgart, 2010): (a) Pneumatically driven direction gyro, Ternstedt Manufacturing Div, GM Corp, Detroit, USA; (b) Electrical direction gyro by Siemens-LGW, Berlin, Germany; (c) Direction gyro S.F.I.M by BEZU, France; (d) Gyro compass of Anschuetz, Germany; (e) Artificial Horizon, Manufacturer not known; (f) Electrical Turning Pointer by Apparatebau Gauting, Germany.

In 2017, the German Federal Ministry of Education and Research (BMBF) awarded a grant for a project of the 3D digitization of this collection. The project is called *Gyrolog* (from the Greek γύρος, rotation, and λόγος, teaching). Its aim is to use digital methods (see Sections 4 to 6) to free the inconspicuous, yet highly complex objects of the today's ubiquitous gyro technology from their black box in order to open this technology for research in history of technology, technology didactics, museum education etc. as well as for teaching in schools, universities, and institutions of further education. Digitization also makes this technology understandable in the truest sense of the word - virtually - and can be researched by the disciplines mentioned after the project has been completed towards the end of 2020.

Furthermore, the virtual character of the digitized collection enables the option of reuniting the collection with its historically formed subsidiaries at the Technical University of Munich, Germany, and the Johannes Kepler University of Linz, Austria. Additional instruments like an original copy of the

Preprints (www.preprints.org) | NOT PEER-REVIEWED | Posted: 8 December 2020 doi:10.20944/preprints202012.0205.v1

Machine of Bohnenberger, which is described in more detail in Subsection 6.1, can also be added virtually.

4. Two-dimensional Data Collections and Postprocessing

Meanwhile, the digitized collection of gyro instruments can easily be accessed by 2D pictures. This human-computer interaction (HCI) interface provides first details of these highly complex and fascinating objects.

Accordingly, the intention behind the 2D digitisation was to provide the user with as many views as well as details of the gyroscopic instruments as possible. However, compared to the newly created 3D objects, 2D pictures always provide limited object details depending on the Field-of-View. The Gyrolog 2D setup is based upon photographic studio facilities, with a professional background and lighting. A light crème colour was chosen as background to contrast with the mostly dark, black or metallic objects.

For the 2D data collection process a standardised procedure was created that included fast response and digitisation time as well as an elaborate way of handling the objects to minimise the impact of the data collection. First, the object is placed on the 2D set-up for the so-called characteristic view, which was developed together with a professional photographer. This characteristic view will guarantee a first impression with all relevant information contained within the gyro instrument in one view, if possible as seen in Figure 5a.

Figure 5a. Characteristic view of the artificial horizon with a caging device (inventory number KH22-10, Gyrolog, CC-BY-SA).

Figure 5b. Difficult definition of a front view of a ship gyro compass manufactured by Anschuetz (inventory number GO05/01-10, Gyrolog, CC-BY-SA).

Then the instrument is rotated to see the front of the object. This process includes some challenges with regard to definition. Parts of the gyro collection are aircraft instruments that were built for and used in aircraft cockpits. Here the front view definition is quite easy. Other parts of the collection were rather more challenging but could also be defined together with our collection experts (see Figure 5b). The further data collection process was similarly executed as the object was carefully rotated in predefined ways: the left view, the rear view and the right view. For the bottom and upward view the instrument was cautiously turned. Furthermore, caging devices were used to minimise movements. These were individual fixtures that were partly 3D printed to fit to some of the objects within the collection (see also Figure 5a). In a last step, details such as type labels were digitised for a close-up view. With this data collection process the Gyrolog project ensures a detailed set of 2D pictures from every possible view of the individual gyro instruments.

This 2D dataset was also post-processed after a standardised sorting procedure. The basis for this was laid during the digitisation process. To distinguish between the different views, the 2D digitisation photographer used different coloured labels while digitising the objects to support the post processing. The different labels were colour-coded as well as labelled preserving always the

Preprints (www.preprints.org) | NOT PEER-REVIEWED | Posted: 8 December 2020 doi:10.20944/preprints202012.0205.v1

same order: characteristic view after inventory label, front view after yellow label, and so on, with details and close ups coming lastly after another different white label. During the post processing the pictures were sorted into the different views for each instrument.

For every object, the best pictures are chosen and are available on to the viewing platform Goobi. Goobi [52] is an Open Source web-based software that is used by the University of Stuttgart's library, a Gyrolog project cooperation partner to ensure sustainability of the digital gyroscopes collection (see Section 7).

5. Three-dimensional Data Collections by Means of Computed Tomography, Computer Vision and Endoscopy

With emerging technologies in the fields of data capture, data processing and data visualization three-dimensional object preservations have become state-of-the art in Cultural Heritage, also for Tech Heritage assets. One efficient and robust technology is photogrammetry, using horizontally and vertically overlapping photos for 3D reconstructions of surfaces and hulls. For a long time photogrammetry served for 3D mapping by means of bundle block adjustments and orthophotos. With the invention of DIM, photogrammetry could undergo a renaissance and is equivalent and comparable with geometric computer vision (CV). The photogrammetric bundle block adjustment is the pose estimation of computer vision, also called Structure-from-Motion (SfM). Large image blocks are automatically processed by SfM and DIM algorithms in one software package and deliver finally very dense colored point clouds, which can be meshed for watertight 3D models, also called Virtual Reality (VR) models or Digital Twins (DT).

Endoscopy is using imaging camera systems with huge enlargements but tiny Field-of-Views (FoVs). Therefore it is tricky to collect overlapping image blocks to be accomplished only by controlled camera movements along horizontal and vertical axes. An endoscopic image block can be processed with the same workflow of geometric computer vision, moreover, it can directly be integrated into the CV image blocks which simplifies the point cloud registrations.

CT is also a non-invasive imaging technology providing directly 3D volumetric models or volume elements, in short voxels. As mentioned before, the down-sampling of huge voxel files to come to a reasonable data volumes is quite a challenge, which is needed for the mutual registration process.

The complete 3D contents of our gyroscopes' DTs is obtained by an integration of CT, CV and endoscopy point clouds. CT and CV are co-registered using the similarity transformation as described in section 2. If endoscopic image blocks are simultaneously processed with the exterior image blocks, then they are automatically co-registered. If not, another similarity transformation ought to be accomplished.

5.1. Computed Tomography 3D Data Collection

In comparison to the medical CT machines, industrial ones are more powerful and can easily penetrate through the different alloys of metals. In this work, an X-ray based computed tomography scanner with a resolution in the single digit micrometer range with a photon energy up to 225 KeV is used, see Figure 6.

The goal of the work presented here is to digitize historical gyroscopes and to derive 3D volume data, rather than disassembling them and thus possibly having to destroy them. As usual in computer tomography systems, the 3D volume data shown below were generated by rotating the sample placed on a turntable and taking several thousand X-ray images during the rotation; see Figure 6. From these projections the most widely used algorithm for CT reconstruction, the so-called filtered back projection (FBP) [3], was used. In selected cases, the Maximum-Likelihood Expectation-Maximization (MLEM) reconstruction algorithm is applied with a significantly higher computation time to generate 3D volume data of high quality in terms of noise of the objects [29].

Preprints (www.preprints.org) | NOT PEER-REVIEWED | Posted: 8 December 2020 doi:10.20944/preprints202012.0205.v1

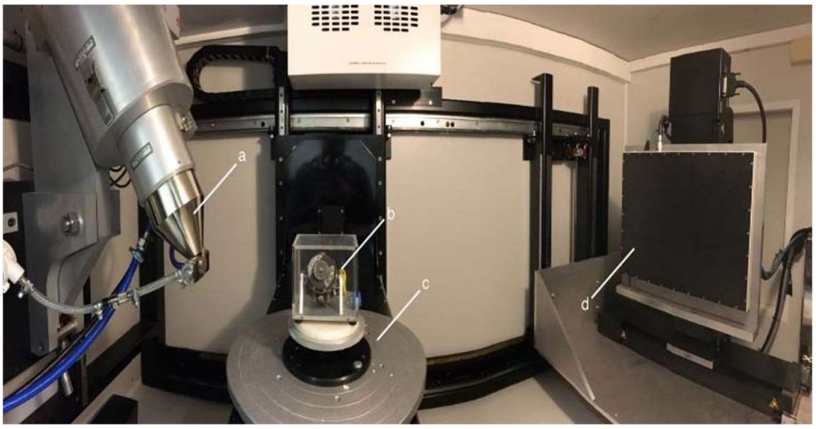

Figure 6. Measurement setup in CT: (a) X-Ray tube, (b) object to be scanned, (c) rotation table and (d) flat panel detector.

There are several noise sources causing artifacts in the 3D volume data. If the imaged gyroscopes are difficult to penetrate by X-rays due to their size and the associated metal content, the projections are contaminated by massive Poisson noise. To tackle this problem, we have applied several denoising techniques to the gyroscope samples. In order to show the results of denoising, the X-ray images were taken with high current and acceleration voltage (Table 1) as a ground truth and later we have simulated the strong Poisson noise over the scanned projections, where approximate number of photons is approximately 500 per detector pixels.

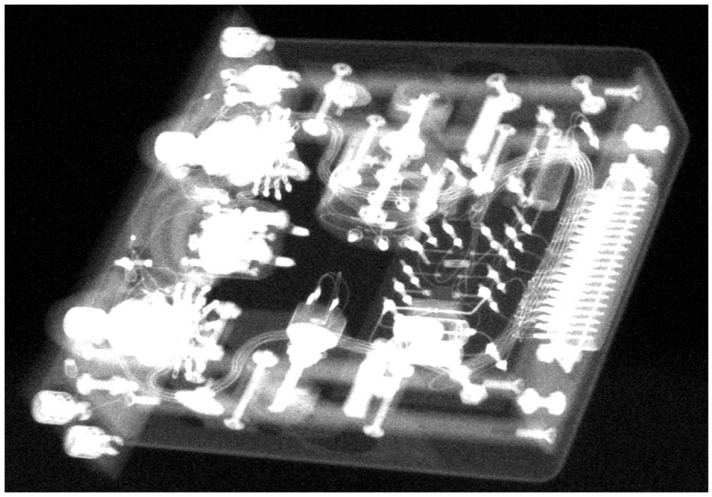

Figure 7. X-ray projection image with simulated and added Poisson noise.

In order to demonstrate this behavior, the target object KH-09-09 was chosen because the object has a massive, closed metal box structure and a large number of small features consisting of mechanical and electrical structural elements, which can be seen in the X-ray projection image in Figure 7.

Table 1. CT scan parameters of KH-09-09 specimen.

X-ray tube voltage	180
Current [μA]	400
Exposure [s]	1
Filter material [mm]	Copper [2.5]
Number of projections	1150

Preprints (www.preprints.org) | NOT PEER-REVIEWED | Posted: 8 December 2020 doi:10.20944/preprints202012.0205.v1

Figure 7 shows that the noise is distributed over the entire projection and thus distorts the fine structure of the image. There are two methods we have used to achieve noise-reduced projections that contribute to the final reconstructed volume. The first denoising method is based on a fully convolutional neural network (CNN) proposed in [30]. The authors clearly show the benefit of the CNN for high Poisson noise being usually the case in computed tomography over the best denoising techniques available in CV for photos with high number of photons and lower Poisson noise. The recently published CNN uses 20 connected layers where 18 of them are using ReLU nonlinearity and two of the last layers are using linear activation function. The architecture, presented in Figure 8, utilizes 64 kernels with size 3x3 to convolve on each layer. The network is trained on real X-ray projections with simulated Poisson noise. It learns the unknown denoising function based on training data. The result of the CNN is shown in Figure 9.

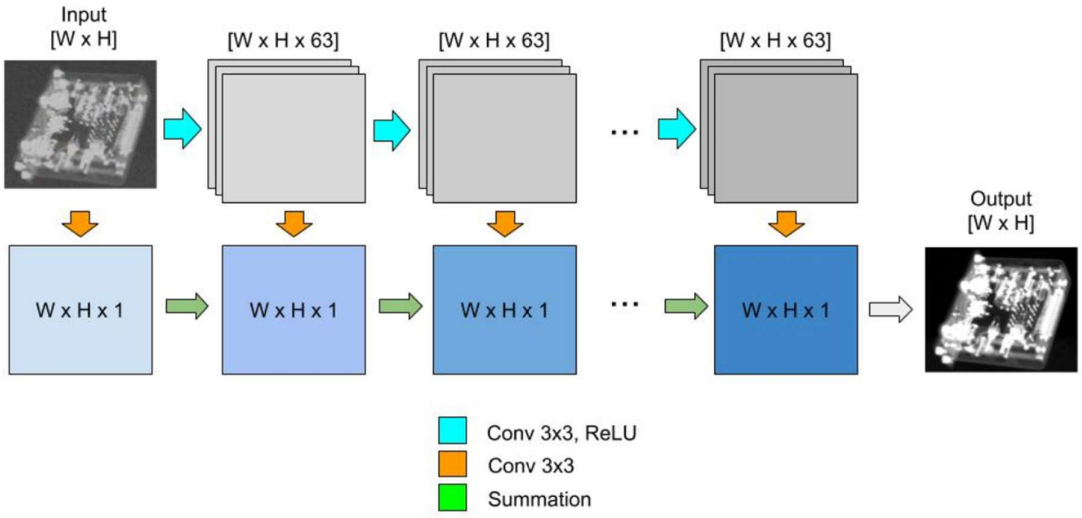

Figure 8. CNN architecture according to [30].

For the MLEM reconstruction we use our implementation combining the penalty which controls the total variation of the calculated volume at each iteration [29] [31] including a regularization parameter β. The scanned specimen KH-09-09 was reconstructed with the regularization parameter β equal to 1e-2 and a total number of 50 iterations. In the cases considered, the MLEM algorithm required about 50 iterations to reconstruct all features of the reconstructed volume. However, if the signal-to-noise ratio of the projections is low, the number of iterations should be more than 50. However, the MLEM algorithm has a computing time of more than 300 hours on a powerful computer with 8 GPUs for the resolution of the detector used here for the projection images with 2300 x 3200 pixels due to the large number of forward and backward projections. In order to reduce the computing time for the reconstruction significantly by a factor of 50 and still achieve high-quality volume data sets with noise reduction, denoised X-ray projections using the CNN architecture of Figure 8 were reconstructed using the FBP. For the learning phase of the network, as ground truth of original high-dose X-ray images, reconstructed 3D volume data sets were generated using FBP. A denoised projection is shown in Figure 9.

Preprints (www.preprints.org) | NOT PEER-REVIEWED | Posted: 8 December 2020 doi:10.20944/preprints202012.0205.v1

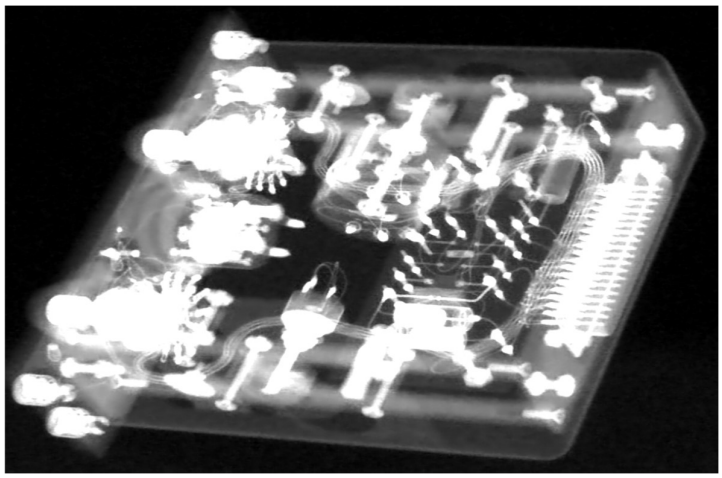

Figure 9. Result of the denoising of KH-09-09 using the CNN of Figure 8.

As can be seen from Figure 10, the results obtained from the MLEM reconstruction of noisy projections and FBP of high dose projections are similar, and in some regions MLEM produces better results, although it is very time consuming. Denoising images with the CNN algorithm helps to remove shot noise for high photon counts. Thus, in comparison to FBP of noisy projections, FBP of denoised projections shows better overall results. The noise error for both methods can be calculated assuming the FBP of original projections without noise as a ground truth. Thus, the following metrics can be used such as the peak-to-signal-noise-ratio (PSNR), mean-squared error (MSE) and signal-to-noise-ratio (SNR).

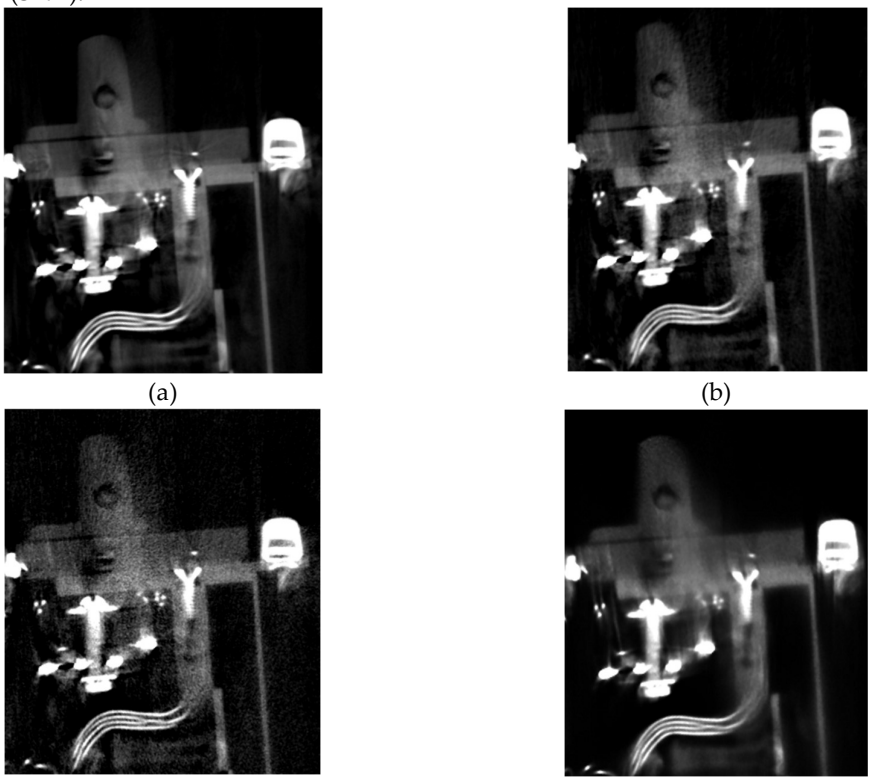

(a) (b)

(c) (d)

Figure 10. Region of volume KH-09-09 reconstructed: (a) FBP of high dose projections; (b) FBP of denoised projection by CNN architecture of Fig. 8; (c) FBP of noisy projections; (d) MLEM of noisy projections.

Preprints (www.preprints.org) | NOT PEER-REVIEWED | Posted: 8 December 2020 doi:10.20944/preprints202012.0205.v1

For the second object G200, we have generated the iso-surfaces for both the denoising technique of the CNN architecture of Figure 9 and the iterative reconstruction algorithm MLEM and one surface for the original high dose scan. Compared to the first experiment, the Poisson noise will not be added to the projections. Thus, the reconstructed object will suffer from beam hardening and scattering artefacts and shot noise. The scan parameters for the G200 specimen are given in Table 2.

Table 2. CT scan parameters for object G200.

X-ray tube voltage [kV]	170
Current [μA]	740
Exposure [s]	1.4
Filter material	Copper [4.5]
Number of projections	1256

The outer and inner structures of G200 are complex. On the surface there are several cables and pins which cause more streak artefacts as the walls of the object are thick, difficult to penetrate by X-rays and made of different metal alloys such as iron, copper and aluminum. The main goal before scanning was to use high energy and metal filters to harden the X-ray beam and prevent highly visible artefacts coming from the polychromatic nature of the source. Therefore, the copper filter with a thickness of 4.5 mm was used to reduce the beam hardening artefacts and exposure time of 1.4 s to receive more photons on the detector. The surface renderings [33] [34] and iso-surfaces of the G200 object are depicted in Figure 11. As is obvious, the reconstructed volume based on the FBP has severe artefacts both on the outer and inner surface.

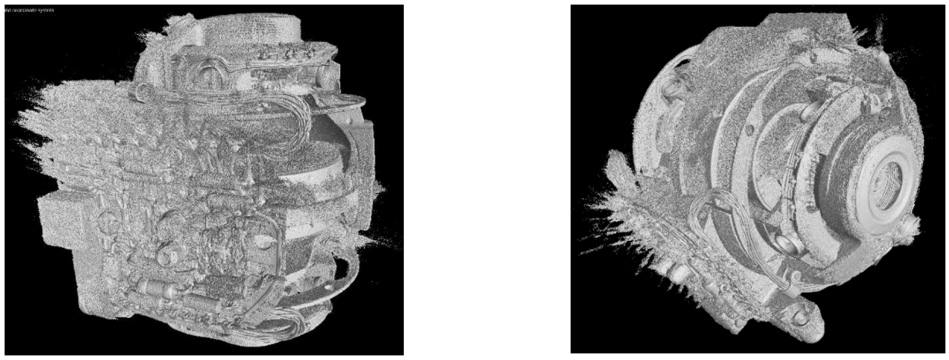

Figure 11. Two views of the iso-surface of G200 from the 3D volume data set reconstructed by the FBP.

Figure 12 shows the difference in iso-surfaces generated from the reconstructed volume from the denoised projections calculated by the CNN. The noise and metal artefacts are significantly reduced compared to Figure 11, where the denoising technique was not applied.

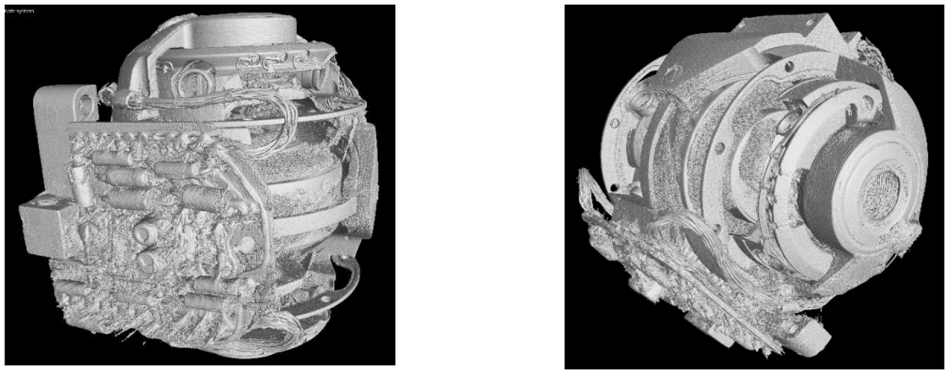

Figure 12. Two views of the iso-surface of G200 calculated from the 3D volume data set reconstructed by the FBP from the denoised projections.

Preprints (www.preprints.org) | NOT PEER-REVIEWED | Posted: 8 December 2020 doi:10.20944/preprints202012.0205.v1

In comparison to Figure 11, Figure 13a has been reconstructed by down-sampling projections by a factor of 4. The quality of the iso-surface is further significantly improved, due to the increased signal-to-noise-ratio produced by the down-sampling process in each dimension. This factor of 4 results in an increase in the number of photons of 64 per voxel in the 3D volume enhancing the signal-to-noise-ratio in dB by a factor of 8, which is also the reason for the overall quality improvement of the iso-surface in Figure 13b compared to Figure 12a and b. The reduction of the spatial resolution by down-sampling is no limitation in the context of the CT images considered here, since voxel sizes in the one to two-digit micrometer range still have a sufficient resolution of 100 of the 150 micrometers by down-sampling by a factor of 4 and possibly even more. This resolution is no limitation for the use of the data to visualize the objects including their internal structures in the context of digital heritage. The denoised projections based FBP reconstruction of Figure 13b shows the best overall results of all considered cases. Obviously, based on the iso-surface we can relatively and accurately differentiate the structure of the square and the circular region-of-interest (ROI) being part of the electronic components and the rotor shape, respectively.

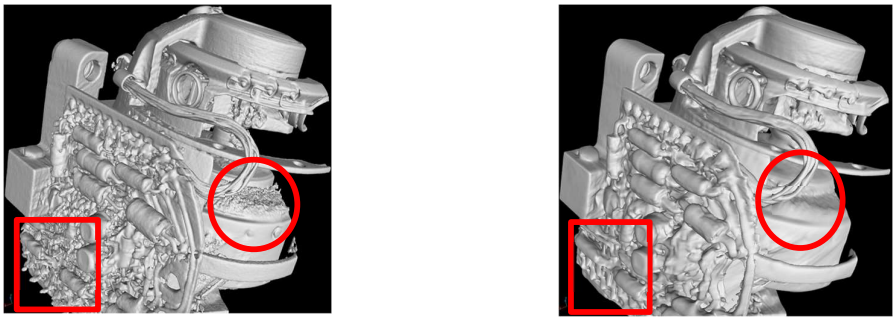

(a) (b)

Figure 13. Comparison of two iso-surfaces calculated from reconstructed volumes in the ROIs: (a) from original projections; (b) from denoised projections.

Based on the methods just described, 3D models of the gyroscopes in the collection were generated. Exemplarily, parts of the Machine of Bohnenberger (see subsection 6.1) are reconstructed and shown in Figure 14. The structure of the inner rod can be clearly seen by a cross-sectional image through the 3D volume data set in Figure 14b. In addition, a further segmentation with predefined material threshold results in the entire surface of the gyroscopic gimbal in Figure 14c, with the exception of the spherical ivory structure.

(a) (b) (c)

Figure 14. The Machine of Bohnenberger and CT scans: (a) Photo; (b) Cross-sectional view of the CT scan of the inner rod; (c) Gimbal iso-surface of the CT scan.

Preprints (www.preprints.org) | NOT PEER-REVIEWED | Posted: 8 December 2020 doi:10.20944/preprints202012.0205.v1

5.2. Geometric Computer Vision and Photogrammetric 3D Data Collection

The principle of three-dimensional (3D) point reconstruction from imagery is called triangulation (see Figure 15). An object is captured in at least two different photos and the corresponding image point coordinates of p_1 and p_2 are measured. With additional camera orientation information for O_1 and O_2 (image poses) the 3D corresponding point P can be calculated by forward intersection.

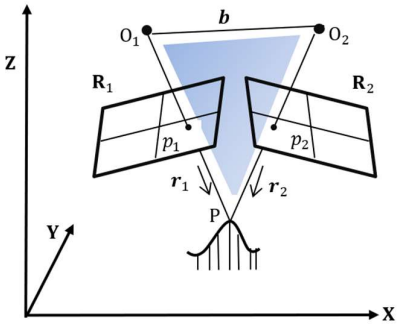

b - displacement vector between two perspective centres
$\mathbf{r}_1$ - vector from image point to object point left image
$\mathbf{r}_2$ - vector from image point to object point right image
$\mathbf{R}_1$ – rotation matrix of left image wrt object coordinates
$\mathbf{R}_2$ – rotation matrix of right image wrt object coordinates

Figure 15. Basic principle of 3D point reconstruction using images – geometry of coplanarity

The 2D-3D correspondences can be either expressed by the collinearity equations in photogrammetry

$$x - x_0 = -f\frac{r_{11}(X - X_0) + r_{21}(Y - Y_0) + r_{31}(Z - Z_0)}{r_{13}(X - X_0) + r_{23}(Y - Y_0) + r_{33}(Z - Z_0)}$$
$$y - y_0 = -f\frac{r_{12}(X - X_0) + r_{22}(Y - Y_0) + r_{32}(Z - Z_0)}{r_{13}(X - X_0) + r_{23}(Y - Y_0) + r_{33}(Z - Z_0)} \quad (6)$$

or as the projective equation in computer vision

$$\begin{bmatrix} x \\ y \\ 1 \end{bmatrix} = \begin{bmatrix} f & 0 & x_0 \\ 0 & f & y_0 \\ 0 & 0 & 1 \end{bmatrix} \boldsymbol{R}^T \begin{bmatrix} 1 & 0 & 0 & -X_0 \\ 0 & 1 & 0 & -Y_0 \\ 0 & 0 & 1 & -Z_0 \end{bmatrix} \begin{bmatrix} X \\ Y \\ Z \\ 1 \end{bmatrix} \quad (7)$$

The notation of CV can be abbreviated as

$$\mathbf{x} = \mathbf{K}[\mathbf{R}|\mathbf{t}]\mathbf{X} \quad (8)$$

where $\mathbf{K}$ is the calibrated camera matrix.

In practice, the procedure is split into several steps, as shown in Figure 16. First of all we work with calibrated camera systems, no matter using a D-SLR camera, a camera off-the-shelf or a camera of a mobile device. Camera calibration is an issue for photogrammetry since about 100 years - very precise calibrations for close range applications were proposed in the 1960s. In this project we investigated the performance of camera calibration for four camera systems: the Gyrolog project camera Sony α7R II, a Leica Q and an Apple iPhone 7Plus and a Samsung Note 8 [35]. When extending the ideal lens characteristics with distortion, the collinearity equations (6) are reformulated

$$x - x_0 = -f\frac{r_{11}(X - X_0) + r_{21}(Y - Y_0) + r_{31}(Z - Z_0)}{r_{13}(X - X_0) + r_{23}(Y - Y_0) + r_{33}(Z - Z_0)} + \Delta x$$
$$y - y_0 = -f\frac{r_{12}(X - X_0) + r_{22}(Y - Y_0) + r_{32}(Z - Z_0)}{r_{13}(X - X_0) + r_{23}(Y - Y_0) + r_{33}(Z - Z_0)} + \Delta y \quad (9)$$

Here Δx and Δy are correction terms for image coordinates, r_{ij} are the components of the rotation matrix **R**. With regard to camera distortion, various models are based on either the mathematical principle, the physical principle or the mixed principle. Among many, the classical Brown model and its variants are most widely used [36]. It classifies the distortion into radial distortion Δ_r and tangential distortion Δ_t.

Preprints (www.preprints.org) | NOT PEER-REVIEWED | Posted: 8 December 2020 doi:10.20944/preprints202012.0205.v1

$$\Delta = \Delta_r + \Delta_t \quad (10)$$

In the Brown model, the radial distortion is modeled by the three parameters K_1, K_2, K_3, and P_1, P_2 are tangential distortion parameters. Furthermore, $r = \sqrt{u^2 + v^2}$:

$$\Delta u = u(1 + K_1 r^2 + K_2 r^4 + K_3 r^6) + \left(2P_1 uv + P_2(r^2 + 2u^2)\right) \quad (11)$$

$$\Delta v = v(1 + K_1 r^2 + K_2 r^4 + K_3 r^6) + \left(2P_2 uv + P_1(r^2 + 2v^2)\right) \quad (12)$$

Various methods based on the geometrical relationship are put forward with regard to calibration scenes, calibration models and estimation processes. For this work, experiments are mainly depending on the Matlab® Calibration Toolbox, which uses a plane chess-board.

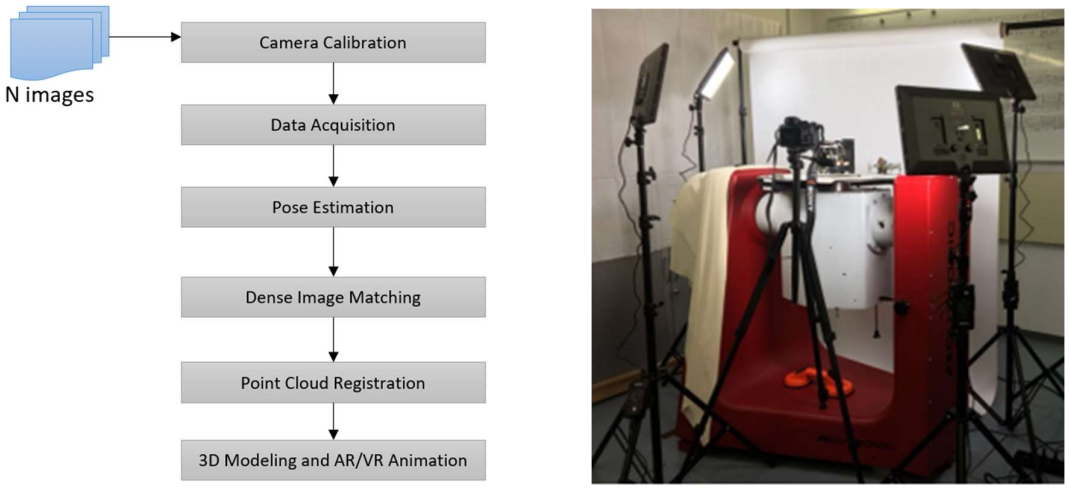

(a) (b)

Figure 16. Data acquisition in the Gyrolog project: (a) workflow of CV/photogrammetry; (b) Gyrolog Lab facility used for photo collections

An example of the the calibrated focal length (pixel) in x direction for the Sony α7R II is shown in Figure 17. For the four calibrated cameras, the Gaussian Fitting Standard Deviations of the calibrated focal length are shown in Figure 18.

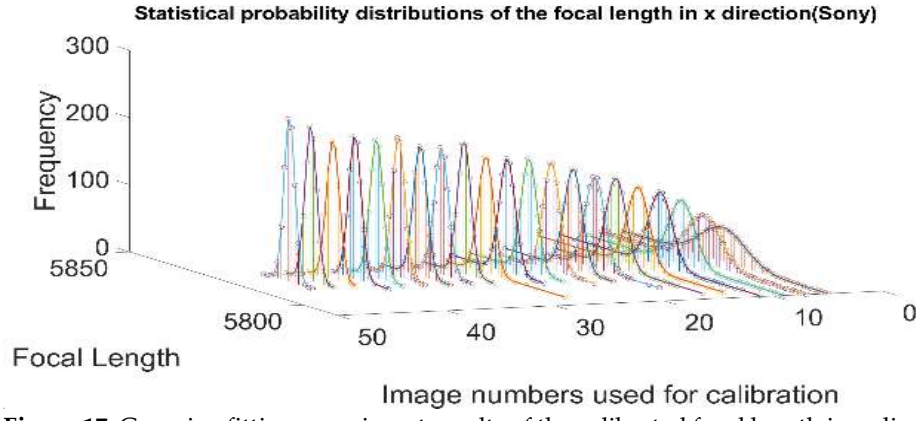

Figure 17. Gaussian fitting experiment results of the calibrated focal length in x-direction Sony α7R II

Preprints (www.preprints.org) | NOT PEER-REVIEWED | Posted: 8 December 2020 doi:10.20944/preprints202012.0205.v1

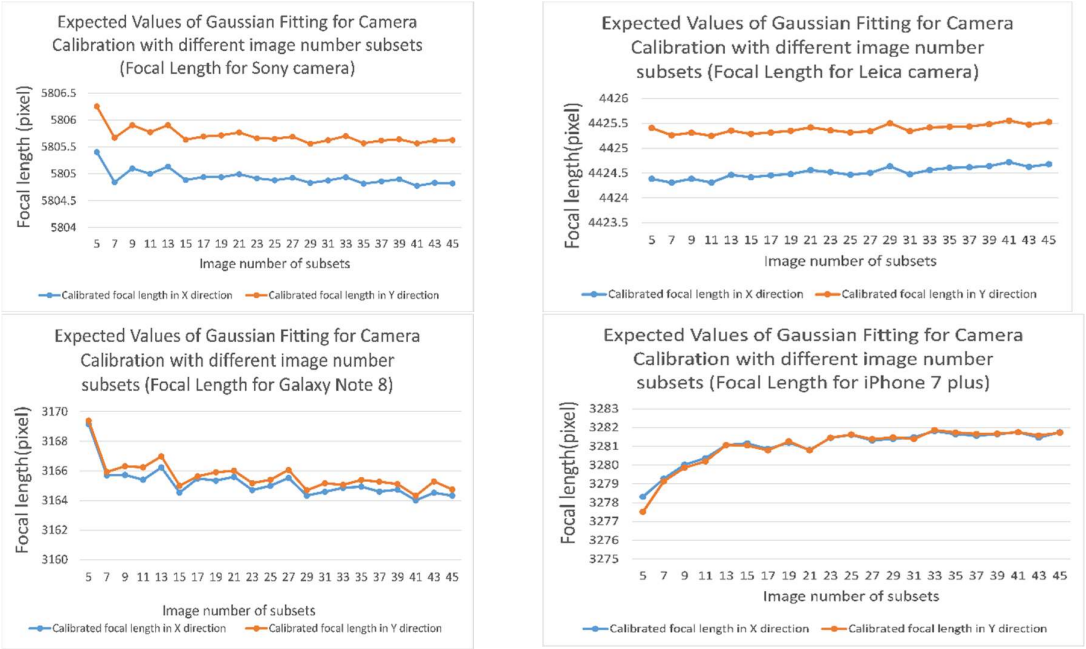

Figure 18. Gaussian fitting standard deviations for the calibrated focal length of 4 camera systems.

After the camera calibration the data acquisition of the gyroscope objects starts. The object to be digitized is placed on a turntable under an appropriate lighting configuration, and the camera is fixed in a suitable position to take pictures, while rotating the turntable with a certain speed. With 500 to 800 images from all views in horizontal and vertical modes, and after estimating the camera pose using SfM, a dense point cloud can be calculated by dense image matching for further 3D modeling processes or VR/AR (Virtual and Augmented Reality) animation. When the calculated 3D model is not complete, most probably due to the lack of information from invisible perspectives, additional images need to be taken and the corresponding point clouds will be integrated with the previous ones to complete the model. This process is called point cloud registration and part of Figure 16a. A first successful test coloring 3D CT scans with photo textures is given by [37].

5.3. Endoscopy in 3D

An endoscope is an illuminated optical, typically slender and tubular instrument. The lens projects a real life scene image onto the first focal plane, which is then transmitted by the reversal system to the final focal plane. At the eyepiece, the image is projected onto the file by a camera lens. An example of an endoscope can be seen in Figure 19.

Figure 19. Structure of an endoscope. © Karl Storz SE & Co KG)

Specialty for endoscopes Among all steps, a proper data acquisition delivers the biggest difference with normal camera applications. Rather than just for visualization, more factors of an endoscope

Preprints (www.preprints.org) | NOT PEER-REVIEWED | Posted: 8 December 2020 doi:10.20944/preprints202012.0205.v1

should be taken into account, such as accuracy, image quality, appropriate imaging block, and many more. In traditional 3D reconstructions within CV and photogrammetry, the overlap between neighboring images should be over 80%, because of the imaging distance and resolution. A D-SLR or off-the-shelf camera can fulfill the requirement without much effort, however for an endoscope, the situation is quite different (see Figure 20).

(a) (b) (c)

Figure 20. Endoscopic imagery: (a) opening angle; (b) mechanical gimbal set-up; (c) image

Suppose the imaging distance is d, the coverage of the object space can be calculated via

$$I = 2d * \tan(\alpha/2) \quad (13)$$

In our case, the viewing angle is 75° and the imaging distance is ranging from 5-15mm. Therefore l can be determined from 8-23mm. If we need 80% overlap between neighboring images, the movement of the tip should be 1.6 - 4.6mm, which is extremely difficult to accomplish in reality while operating the endoscope to collect image blocks.

Due to the challenging imaging characteristics stated above, a suitable endoscope type should be chosen to ensure invasive possibility and sufficient image quality. In addition, only using images as input for pose estimation requires suitable image configurations, especially the overlap between neighboring images. The endoscope holder can be either mechanical, which gives less automation, or normally more expensive, a robotized device. Since highly precise movement control is hard to reach in practice, streaming video can be used instead of taking still images. In practice, though video frames deliver lower resolution than endoscopic still images, highly overlapped extracted frames can make the image alignment task much easier. Even with streaming video as input for 3D reconstruction, there are still several precautions.

Experiment setup Instead of using free hand movements, a more stable solution is proposed with a self-designed gimbal. The fixture has 4 degrees of freedom. The whole system consists of several parts: for horizontal movement, a cross slide is used as the base, and another single slide is attached via a 3D printed 90 degree adapter with the cross slide. In addition, a ball head is fixed for the rotation movement. With this assistant, it is possible to use screws to calmly move the endoscope for enough overlap between the images. The endoscope is able to move forward and backward, left and right, up and down and laterally as well with the assistant device.

The movement of the gimbal-assisted endoscope is shown in Figure 21. Here a total of about 200 overlapping endoscopic images have been processed to deliver a colored point cloud – the software used for SfM and DIM is RealityCapture.

Preprints (www.preprints.org) | NOT PEER-REVIEWED | Posted: 8 December 2020 doi:10.20944/preprints202012.0205.v1

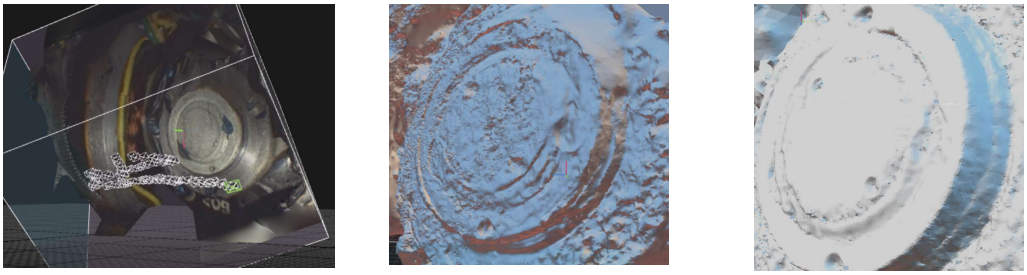

(a) (b) (c)

Figure 21. An endoscopy 3D mesh aligned with RealityCapture: (a) Alignment; (b) meshed point cloud; (c) meshed point cloud by CV/photogrammetry

Finally a comparison of 3D meshes generated by endoscopic and photogrammetric image blocks could be accomplished (Figure 21b and c). Due to the enlargements of the endoscopic camera systems more details can be resolved than with regular D-SLR or off-the shelf cameras, which might be important for historical research of a gyro system. Working with endoscopic image blocks is a challenge. With the self-designed mechanical gimbal the generation of densely colored point clouds has been proven to be feasible. Further experiments will follow to explore the full potential of multi-view stereo of large endoscopic image blocks.

6. Digital Twins of the Gyroscope Collection - Examples

6.1. The Machine of Bohnenberger – The Very First Gyroscope

In 1810, the astronomer, mathematician and physicist Johann Gottlieb Friedrich Bohnenberger (1765-1831) invented the gyro with cardanic (or gimballed) suspension at the University of Tuebingen in south-west Germany [26]. This instrument served initially as a teaching tool during his lectures in astronomy. Bohnenberger used it for demonstrating the orientation keeping of the Earth rotation axis during the Earth's yearly journey around the sun as well as for demonstrating the precession motion of this rotation axis. (The latter is a periodic movement with a duration of about 25.800 years while the axis describes the surface of a double cone. This effect leads to a slow circular motion of all fixed stars at the night skies with that long period.). Bohnenberger described systematically the design and the use of that instrument for the first time [38].

Based on the details of Bohnenberger's paper, it was possible to discover two original copies at a school in Tuebingen in 2004 and during an internet auction in 2010 – the only still existing originals known to the authors. These findings were reason for some historic research about the early dissemination of the instrument and its contribution to modern gyro technology: Probably in 1812, Bohnenberger had already sent two copies of the instrument to P.S. Laplace and the Ecole Polytechnique in Paris, respectively. In subsequent years this apparatus was introduced in the physical collections of many French schools. Therefore, L. Foucault knew that device very well. During his investigations on a simple experimental proof for the rotational motion of the Earth he improved Bohnenberger's invention and called it Gyroscope, because he could not get a sufficient approval of the specific property of his well-known pendulum, which can sense only the vertical component of the Earth's rotation rate [39]. A gimballed gyro, however, is at least theoretically applicable for measuring the full rate. Although technical imperfections prevented Foucault from being successful with this approach, his work opened the development of important navigation instruments. In particular, the gyro compass, artificial horizon, and directional gyro (leading also to contemporary inertial and integrated navigation systems) [25][26]. Furthermore, it is this success of the gyro with cardanic suspension which stimulated decisively the development of Laser gyros and fiber optical gyros as well as micro electro-mechanical (MEMS) gyroscopes as a mass product of today.

The Machine of Bohnenberger is virtualized in 3D by a combination of 3D CT scans and 3D CV colored point clouds, using the similarity transformation of section 2. In total, about 500 photos are

Preprints (www.preprints.org) | NOT PEER-REVIEWED | Posted: 8 December 2020 doi:10.20944/preprints202012.0205.v1

taken with the Sony α7R II D-SLR camera and processed by AgiSoft's PhotoScan, now Agisoft Metashape, and Capturing Reality's RealityCapture software packages. A comparison of both photo alignment and DIM softwares shows a clear advantage for RealityCapture, as this software is faster and resolves for DIM in critical lightening conditions. The 3D digital twin is on display in Figure 22.

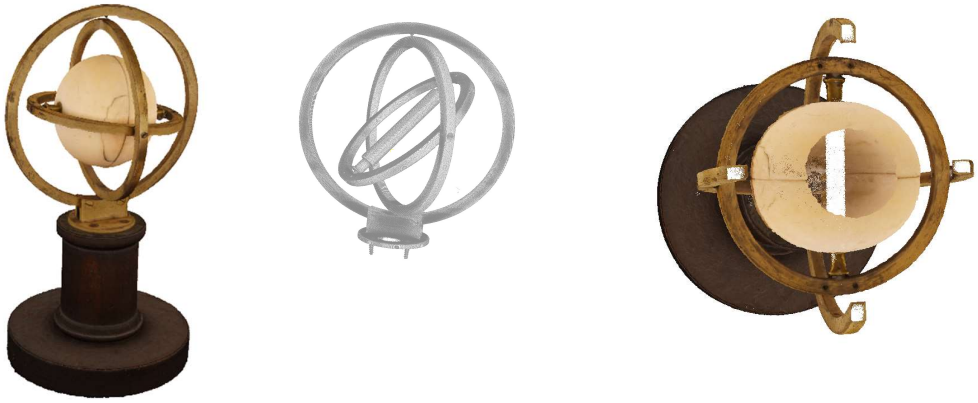

(a) (b) (c)

Figure 22. 3D digital twin of the Machine of Bohnenberger: (a) meshed point cloud of CV/photogrammetry; (b) iso-surface of the gimbal CT scan; (c) split view of CT&CV integrated model.

This digital twin of the Machine of Bohnenberger can be used for Augmented Reality and Virtual Reality animations and also for reverse engineering and 3D printing. In addition, it can be easily decomposed into its basic components by 3D Constructive Solid Geometry (CSG) modeling, for which every CSG feature can be semantically enriched to provide an overview of the functions and materials.

6.2. Directional Gyro LKu4

A rather different example for bringing a mechanical gyroscope alive is the directional gyro LKu4 manufactured by Siemens. This instrument was built during the 1930s and 40s in Germany, thus being one gyro instrument that was used extensively by the German Armed Forces during World War 2 (WW2). Furthermore, it makes the introduced directional gyro an early example of mass-produced gyro instruments within Germany's wartime production. In the Stuttgart collection one finds many such examples of objects such as these. There is an unaltered one (KK02-09), a cut open one (KK12-09) to show students the inside and the working principle of the instrument as well as an altered one (KK09-09) showing the object in running conditions. In addition, there is another model available being used for a research project of a diploma thesis [40] (KK34-20) and several other objects (KK17-09, KK22-09) containing parts of this kind of directional gyro. These different usages of a gyro object demonstrate a distinguishing feature of university collections with regard to museum collections: the use in research and teaching.

To follow the path of these objects one has to start historical research with the object or its digital twin, as there is nearly no written information preserved giving testimony about their origin or their use before they entered the Stuttgart collection. Due to Oral History Interviews conducted as part of the Gyrolog project we know that some Siemens objects might have come from surplus war material directly from the Siemens Company, after the WW2. The university institute, in which the collection was established during the 1960s was located right next to the Siemens building [41].

The LKu4 was part of a range of products produced by Siemens during WW2. It and all the different variations were widely used within the German Airforce, for example in some versions of the Heinkel He111 and Junkers Ju88 [42] (see Figure 23a). It was one of the first electrical powered directional gyros (in comparison for example to the pneumatical directional gyro mainly used by the

Preprints (www.preprints.org) | NOT PEER-REVIEWED | Posted: 8 December 2020 doi:10.20944/preprints202012.0205.v1

American Air Force and could also be used as a part within a yaw axis control mechanism. Thus, this object is a good example of different technological developments in different countries. Siemens pointed out the advantages of electrical driven gyros in its advertisement (see Figure 23b), e.g. the risk of freezing in higher altitudes [44] is reduced. The Stuttgart object is displayed in Figure 23c.

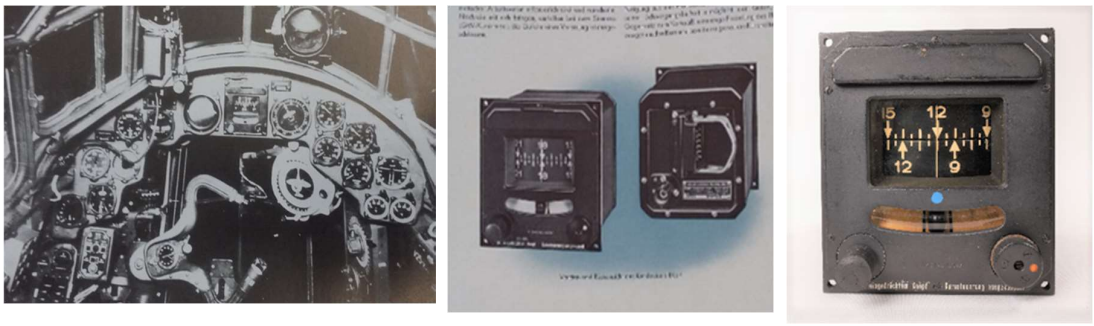

(a) (b) (c)

Figure 23. The LKu4 by Siemens: (a) mounted in a Junkers JU 88 A-1 cockpit; (b) Siemens ad from the early 1940s; (c) front view of Gyrolog asset.

As the LKu4 has transparent and mirroring material at the front the CV/photogrammetry 3D reconstruction process is a bit different from the conventional workflow. Here we use not only ordinary photos taken with the turntable, but also sprayed front-view images. After the data acquisition, all image poses are estimated together in the same coordinate system. In the mesh reconstruction phase, ordinary front-view images are deactivated while only sprayed ones are used for the DIM. The result is given in Figure 24b.

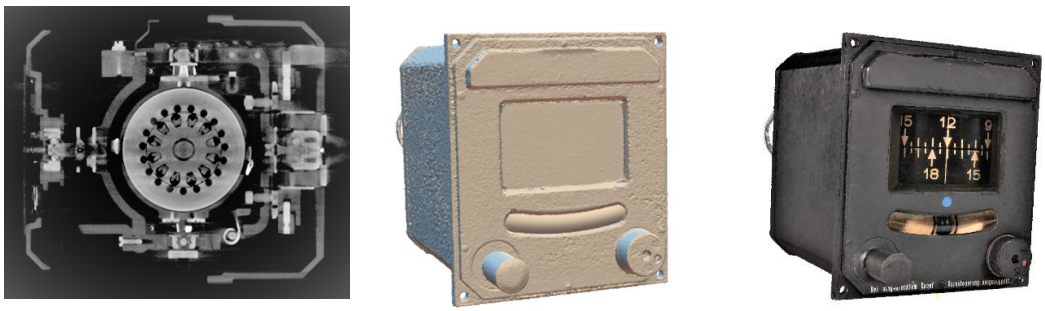

(a) (b) (c)

Figure 24. 3D digital twin of the LKu4: (a) CT scan; (b) CV/photogrammetry point cloud mesh with normal and sprayed images; (c) CT&CV integrated model

Looking at the Gyrolog objects and comparing them with later models one notices that they are all from an earlier manufacturing line (presumably before 1944) as they all still have a bank indicator and internal lighting [45] (see Figure 23c). One can partly trace these timelines when looking at the manufacturer as indicated by the type labels of the objects mentioned above, seen in Table 3. One realizes that these four objects were only produced by two different manufacturers, which actually was the same company, but a different department. In 1936 the „Abteilung für Luftfahrtgeräte“ was established within the Siemens Apparate und Maschinen GmbH (SAM). Between 1936 and 1938 plans were developed to establish a central department within Siemens only for aircraft equipment: the Luftfahrtgerätewerk.

Table 3: Tracing the gyroscopes manufacturers [49]

Inventory number	Manufacturer
KK02-09	Luftfahrtgerätewerk Hakenfelde GmbH, Berlin

Preprints (www.preprints.org) | NOT PEER-REVIEWED | Posted: 8 December 2020 doi:10.20944/preprints202012.0205.v1

KK09-09	Siemens App. u. Masch. GmbH, Berlin
KK12-09	Luftfahrtgerätewerk Hakenfelde, Berlin
KK34-20	hdc (Luftfahrtgerätewerk Hakenfelde, Berlin

The "Hakenfeld" as an addition in the name was added after the location, a part of Berlin-Spandau, where the department was located. The LGW (Luftfahrtgerätewerk Hakenfelde GmbH) was built in Hakenfeld between 1939 and 1941 and officially established as a sub company of Siemens on 1st of October 1940. That means, that all activities under the name SAM were now ceased and realized under the name LGW [50]. That means only KK09-09 was probably manufactured before late 1940, the other three presumably between late 1940 and 1944.

6.3 Gyro G200 of Inertial Platform LN3

Another example is the LN3-G200 gyro of the collection with the inventory number LK05/01-17 (see Figure 25). It was part of an inertial platform, the so called LN3, manufactured by Litton Technische Werke, Freiburg (Litef). The German part of the American Company was founded for the purpose of producing the LN3 platform for the Lockheed F104G Starfighter that was purchased by the German Government during the Cold War Period.

(a) (b)

Figure 25. The Gyro G200 of the LN3 Inertial Platform: (a) Gyro G200; (b) G200 transportation box

This object's story reflects exemplarily lived history of this object of the Gyrolog collection and also traces the links between manufacturer, the state and universities. Thus the object is embedded in this so-called triple helix structure [48] [49]. In 1968 the G200 gyro was being transported in a special transportation box (LK05/02-17) (see Figure 25b) to the Institute of Mechanics at the University of Stuttgart and was supposed to reach Dr.-Ing. Walter Schmid, an associate of the institute. However, it was delivered to Prof. Helmut Sorg on 27th September 1968. Also, part of this delivery were not only these two objects but a folder with information about this particular gyroscope [50]. It contained technical test documents (such as balance tests, gyro torque tests, etc. for different tests benches), which were carried out by Litef during January 1968 until September 1968. Obviously, they were neither carried out for W. Schmid nor H. Sorg nor the University of Stuttgart, but for the Federal Office of Armed Forces Technology and Purchases (Bundesamt für Wehrtechnik und Beschaffung, BWB), an institution of the Federal Ministry of Defence, as the customer. The object shows this as it is indicated in the sources that the object has a BWB number (BWB 1039), a military supply number (6615-00-754-4920) and the information that it came from a military depot (BEL – Bundeseigenes Lager) as well as the indication on the delivery receipt that the G200 gyro was part of an LN3-2A plattform in a F104G. H. Sorg and W. Schmid were both members of the initial institute that started this collection under the direction of Prof. Magnus. In 1968, Prof. Sorg was the interim head of the institute during an interims period when Prof Magnus left to the Technical University of Munich. W. Schmid finished his dissertation [43] as well as the report for the German Science Foundation (DFG) on the same topic in December 1967.

Preprints (www.preprints.org) | NOT PEER-REVIEWED | Posted: 8 December 2020 doi:10.20944/preprints202012.0205.v1

Due to these objects and the archival sources one has a starting point for historical research into the connections between the research, manufacturing and use of gyro instruments in the 1960s in the German Federal Republic. The G200 gyro can be placed in a wider context of a complex structure between three branches within the development of this technology, a university (University of Stuttgart), an industrial manufacturer (Litef) as well as the German Federal Republic, here in form of its military branch (BWB – Ministry of Defence).

The 3D digitisation of this object and the historical contextualisation was only one step in bringing this gyroscope object back to life. The next step was the 3D modeling to animate its functional principle in an AR smartphone application. This means that the object is rebuilt digitally based on the 3D data generated by the Gyrolog project. This 3D modeling project is being carried out as a Master's Thesis within the Digital Humanities Department at the University of Stuttgart. As is well-known, the G200 gyro is situated in the complex story of the Starfighter-Affaire, an interesting and a media-savvy political drama within Germany's Cold War history [51]. This, as well as its functional principles as a black box navigation tool, makes these instruments also very interesting for history of science and technology museums. The Gyrolog project together with the Master's Thesis cooperates with the Deutsche Museum, Munich, that will incorporate this final 3D App in its new tour after the reopening of the aircraft exhibition, thus bringing this gyroscope digitally back to life for many visitors from all over the world.

The 3D digital twin of the G200 Gyro is on display in Figure 25, with 25a the 3D CT scan, 25b the 2.5D CV/photogrammetry reconstruction and 25c a split view into the CT/CV integrated 3D model.

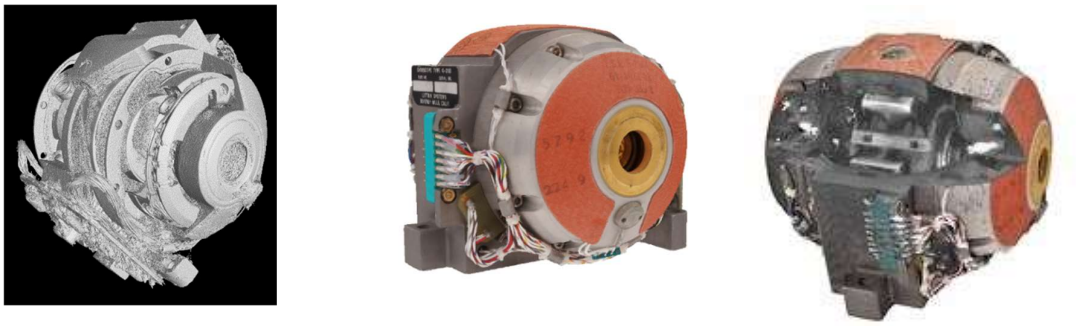

(a) (b) (c)

Figure 26. 3D digital twin of the DM-LN3-G200 gyro: (a) iso-surface of a denoised FBP CT scan (b) meshed point cloud of CV/photogrammetry; (c) split view of CT&CV integrated model.

6.4 Two more examples of Gyrolog 3D Digital Twins

In order to demonstrate our workflows and capabilities we are able to produce 3D digital twins of all sizes of TH assets in a box range of up to $0{,}3^3 m^3$ size. Our gyroscopes have a max. size of $0{,}1^3\ m^3$ with very complex structures, such as metal sheets, wires, electrical drives and servos, etc. The view into the TH object can be accomplished without any difficulties using OS libraries, e.g. CloudCompare, MeshLab, PCL, etc.

In Figure 27 the pneumatically-driven gyro, manufactured by Ternstedt Manufacturing Div., GM Corp., Detroit, USA (see also Fig. 4a) and the electrical direction gyro, manufactured by Siemens LGW, Berlin, (see also Fig. 4b) are on display. Looking at all three views: the internal view obtained by CT scans, the CV/photogrammetry external view and the split view of the integrated model underlines the complexity of the gyro instruments.

Preprints (www.preprints.org) | NOT PEER-REVIEWED | Posted: 8 December 2020 doi:10.20944/preprints202012.0205.v1

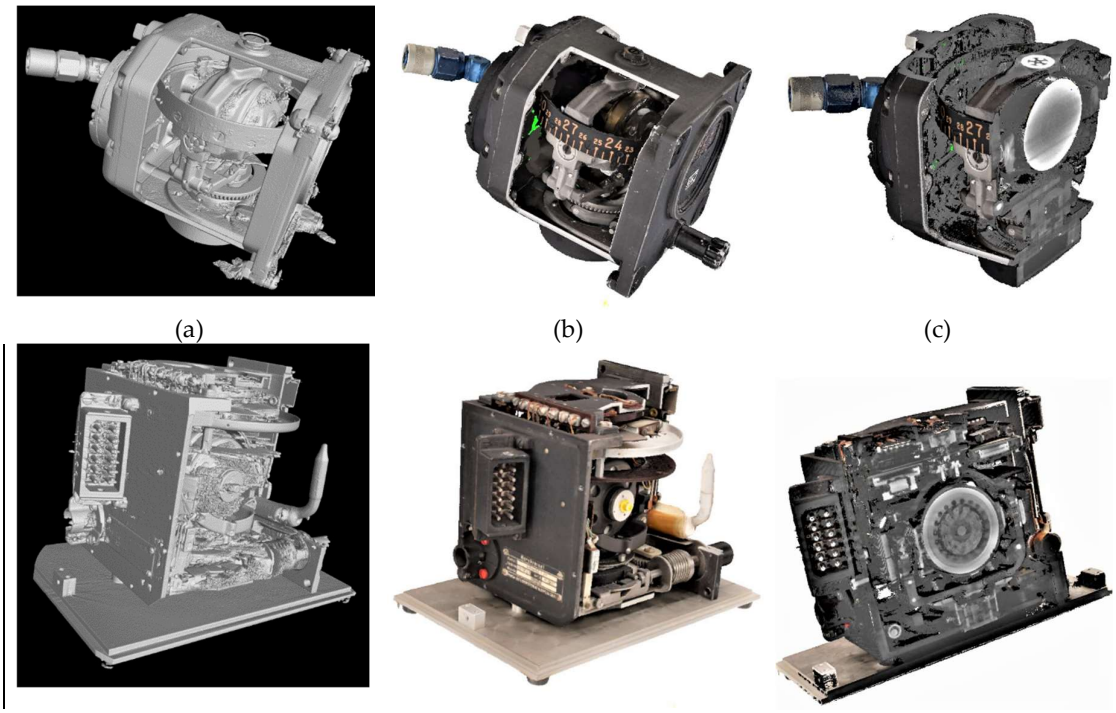

(a) (b) (c)

(d) (e) (f)

Figure 27. Two more 3D digital twins of the Stuttgart Gyroscope collection – the Ternstedt direction gyro (a-c) and the Siemens direction gyro (d-f): (a, d) iso-surfaces of denoised FBP CT scans; (b,e) meshed point clouds of CV/photogrammetry; (c,f) split-views of CT&CV integrated models.

7. Curation of Gyrolog and Open Access

Stable long-term accessibility of both the digitized objects as well as their pertinent metadata are decisive prerequisites for sustained usefulness of all digitization efforts – otherwise invisible objects would merely be replaced by hidden or, even worse, lost digital data. In the Gyrolog project sustainable data curation rests on four pillars addressing the technical and the formal as well as the administrative aspects of longtime accessibility.

First of all, the Gyrolog project maintains a strategic partnership with the university library to grant stable availability of the digitized objects. This institution has already accumulated considerable expertise with 2D digitization of books, architectural drawings, maps, and the like. The library presents its digitized resources via the viewing platform Goobi [52]. Goobi is an OS web-based software providing both the front end viewer as well as the back end digitization management system. In order to present the Gyrolog data, the viewer has recently been expanded to 3D representations (see Figure 28).

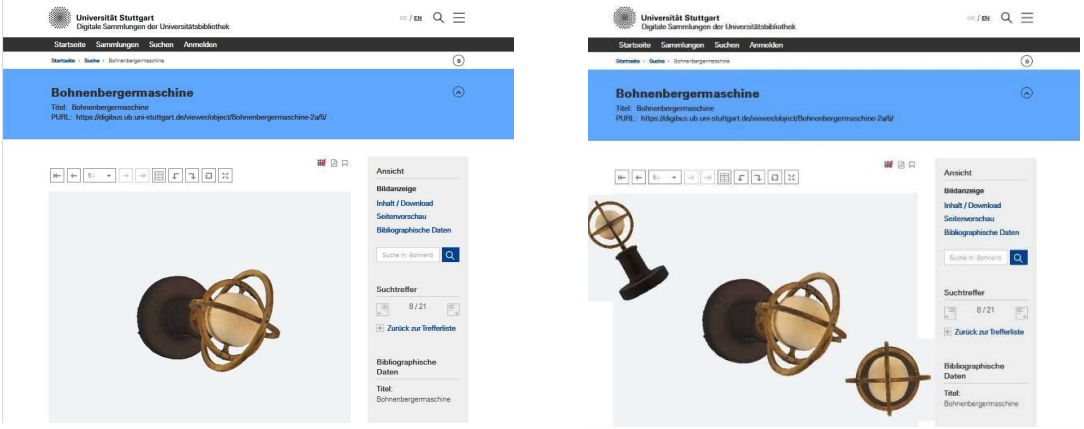

Figure 28. The Machine of Bohnenberger in two successive screen shots

Preprints (www.preprints.org) | NOT PEER-REVIEWED | Posted: 8 December 2020 doi:10.20944/preprints202012.0205.v1

It uses gltf files for graphics output whereas obj files are used in Goobi's internal workflow. A difficulty that occurred during the implementation points to a characteristic dilemma of digitization: digitalized objects become unmanageable if they are too detailed because data files will become too big for comfortable consultation. The huge obj files are significantly compressed when being turned into gltf files, but in most cases additional compression via the open source compression library DRACO has proven indispensable to ensure smart user experience. Gyrolog is the pioneering project for Goobi's enhanced functionality and it is expected that several other university libraries will follow. Contrary to museums, university collections in Germany usually have no permanent professional IT personnel of their own and often are an institutional subunit with the local university library anyway.

Whereas Goobi's curated data workflow allows for both 2D and 3D representations including the pertinent metadata, Gyrolog's massive amount of research data is hosted by DaRUS, the University of Stuttgart's data repository for long-time data storage and accessibility. Via DaRUS, which forms the second pillar for Gyrolog's longevity, all available 2D data as well as the CT and CV/photogrammetry data will remain accessible for at least 10 years. This would enable researchers in the future to reprocess point clouds e.g. with novel algorithms. The file system strictly refers to the objects' inventory numbers and allows for the unambiguous attribution of every data set to the original object. This is all the more important as data come from many different sources and in different formats. The inventory thus forms the data hub of Gyrolog's metadata stock, the third pillar of long-term searchability. Apart from the images' pertinent technical metadata it contains semantic metadata providing information on the respective object's manufacturer, its life cycle and many more aspects. Curating the data comprehends the development of controlled vocabulary – for example the common labelling as "gyro" obviously is no help for the differentiation of the objects in the collection and a more finely grained classification had to be developed. This was done in cooperation with the Deutsches Museum at Munich, another facility holding a major collection of gyros in Germany. The unambiguous identification of manufacturers, corporations and scientists/inventors is achieved by reference to the Integrated Authority File (German: Gemeinsame Normdatei GND) [53]. Conceptual conformity with the CIDOC Conceptual Reference Model and meta data format interoperability with major web portals such as *Europeana* (via the Deutsche Digitale Bibliothek to which Goobi exports data routinely) allow for maxímum accessibility of Gyrolog's digital data.

Accessibility, finally, refers not only to formal issues such as controlled vocabulary and to technical aspects like longtime data storage but also to the legal situation. Here open access (OA) is the fourth pillar of Gyrolog's sustainable data curation. All gyrolog data and metadata are shared under the Creative Commons licence CC-BY-SA. Open access was not only a formal requirement for the grant but is also requisite for the intended broad use of the digital twins in teaching and research, for example in the history of technology or for visualization purposes in courses on mechanics. Moreover, crowdsourcing has become a substantial human resources supply in developing cultural heritage [54]. There are so many knowledgeable gatherers and enthusiasts of gyro instruments whose expertise might prove valuable in filling the gaps in our knowledge of our objects and of gyro history more generally. To get to know these experts and to encourage them to contribute to Gyrolog's semantic metadata is an exciting task that is only beginning as we approach the termination of the proper digitization process.

8. Conclusions and Outlook

This paper has demonstrated, that 2D, 2.5D and 3D digitization of Tech Heritage objects is a challenge and can be mastered combining different technologies. For our application, to sustain the Gyroscope collection of the University of Stuttgart, we used Computed Tomography, geometric Computer Vision, Endoscopy and Photogrammetry. First, all objects are 2D photographed and labelled, just for archival purposes. The real challenge is the generation of Digital Twins in 3D. As is well-known, CT delivers 3D voxels of superb resolution, much higher than the Ground Sampling Distances (GSDs) of CV and photogrammetry. Thus, a decision was made to resolve CT models with similar GSDs as CV/photogrammetric point clouds with denoising characteristics. It was also proven, that endoscopic

image blocks can be aligned in one Structure-from-Motion processing step, to estimate the poses of all images. This is a big advantage, although the image block data collection using endoscopes is difficult to maintain. After pose estimation disparities for pixel-wise Dense Image Matching are calculated and point clouds are derived. The fusion of CT 3D voxels and CV/photogrammetry 2,5D colored point clouds is accomplished by a Spatial Similarity Transformation embedded in a Gauss-Helmert model of statistical inference. The advantage of this fusion compared with classical ICP solutions is the quality assessment. Here the standard deviations of fused 3D models are clear indicators for the goodness-of-fit of the 2.5D-3D data fusion. The final model is three-dimensional. Finally the 2.5D and 3D Digital Twins are made Open Access in gltf format, using the Goobi platform. Goobi is the standard platform of the Stuttgart University Library, and thus we can guarantee maintenance and sustainability for at least 10 years. This means researchers from all over the world can download the 2D photos, 2.5D and 3D Digital Twins and object semantics for their own research

Our research is a first step into the 3D digitization of Tech Heritage and we are proud of the results achieved. The next steps are the lego-wise decompositions of the complex gyroscopes using Constructive Solid Geometry modeling. So far, we have decomposed simple structures such as the Machine of Bohnenberger and other surveying instruments using Maya, Blender and Autodesk 3ds MAX in time-consuming manual work. A challenge here would be to apply Machine Learning and Deep Learning methods to get similar quality by automatic decompositions compared with manual work. But this will take most probably another decade.

Author Contributions: Conceptualization & methodology: B. Ceranski, D. Fritsch, S Simon and J. Wagner; photogrammetric hardware and software: D. Fritsch & K. Zhan; CT hardware & software: S. Simon & G. Mammadov, endoscopy hardware and software: D. Fritsch, K. Zhan &J.F. Wagner, validation & formal analysis: M. Niklaus, K. Zhan; data curation: J.F. Wagner & B. Ceranski; paper structure & writing supervision: D. Fritsch - All authors contributed to the contents of this article, have read and agreed to the published version of the manuscript.

Acknowledgements: This research was funded by the German Federal Ministry of Education and Research (BMBF), grant number 01UG1774X, and in part by the EU H2020 Program under the grant No. 814596, which is gratefully acknowledged. Special thanks go to Dr. Warren Kenny, Dublin, Ireland, for the language review.

Conflicts of Interest: The authors declare no conflict of interest. The funders had no role in the design of the study; in the collection, analyses, or interpretation of data; in the writing of the manuscript, or in the decision to publish the results.

References

1. Talha, A. & Fritsch, D. Integration of Laser Scanning and Photogrammetry in 3D/4D Cultural Heritage Preservation – A Review. *Int. Journal of Applied Science and Technology (IJAST),* 2019, Vol. 9, pp. 76-91**.** doi: 10.30845/ijast.v9n4p9
2. Jauch, C., Denecke, J., Kühnle, J., Effenberger, I., Hillebrand, J., Kieß, S., & Simon, S. Contactless characterization of electric structures with simulation models based on CT data. *Parameters*, *1*, 2.2017**.**
3. Turbell, H. Cone-beam Reconstruction using Filtered Backprojection. PhD Dissertation. Linköping University Press, 2001.
4. Heinzl, C., Kastner, J. & Gröller, E. Surface Extraction from Multi-Material Components for Metrology using Dual Energy CT. In: IEEE Transactions on Visualization and Computer Graphics, 2007, Vol. 13, No. 6, pp. 1520-1527, doi: 10.1109/TVCG.2007.70598.
5. Brunke, O., Santillan, J. & Suppes, A. Precise 3D Dimensional Metrology using High-resolution X-ray Computed Tomography (muCT). In: *Developments in X-Ray Tomography VII*, SPIE Proceed. 2010, Vol. 7804(1), p. 78040O. doi: 10.1117/12.861354
6. Carmignato, S., Pierobon, A., Rampazzo, P., Parisatto, M. & Savio, E. CT for Industrial Metrology - Accuracy and Structural Resolution of CT Dimensional Measurements. In: *4th Conference on Industrial Computed Tomography (iCT),* 2012, pp. 19-21.
7. Fritsch, D., Wagner, J. F., Simon, S., Ceranski, B., Niklaus, M., Zhan, K. & Wang, Z. Gyrolog—Towards VR Preservations of Gyro Instruments for Historical and Didactical Research. In *2018 Pacific Neighborhood Consortium Annual Conference and Joint Meetings (PNC),* 2018**,** pp. 1-7. IEEE. doi**:** 10.23919/PNC.2018.8579456

8. Morigi, M. P., Casali, F., Bettuzzi, M., Brancaccio, R. & d'Errico., V. Application of X-ray Computed Tomography to Cultural Heritage Diagnostics." *Applied Physics A* 100, 2010, No. 3, pp. 653-661. doi: 10.1007/s00339-010-5648-6
9. Casali, F. X-ray and Neutron Digital Radiography and Computed Tomography for Cultural Heritage. *Physical techniques in the study of Art, Archaeology and Cultural Heritage.* 2006, Vol. 1, pp. 41-123. doi: 10.1016/S1871-1731(06)80003-5
10. Fuchs, T., Wagner, R., Kretzer, C., Schielein, R., Scholz, G., Zepf, M., Bar, F., Kirsch, S. & Wolters-Rosbach, M. Development of a Standard for Computed Tomography of Historical Musical Instruments - the MUSICES project. In: *19th World Conference on Non-Destructive Testing, Munich*. 2016, 8p.
11. Mundy, J. L. The Relationship between Photogrammmetry and Computer Vision. SPIE *Proceed. Integrating photogrammetric techniques with scene analysis and machine vision*, 1993, Vol. 1944, pp. 92-106.
12. Lowe, D. G. Object recognition from local scale-invariant features. In ICCV, 1999, Vol. 2, pp. 1150-1157. doi: 10.1109/ICCV.1999.790410
13. McCarthy, J. Multi-image Photogrammetry as a Practical Tool for Cultural Heritage Survey and Community Engagement. J. Archeological Science, 2014, Vol. 43, pp. 175-185, DOI: 10.1016/j.jas.2014.01.010
14. Hartley, R., Zisserman, A. Multiple View Geometry in Computer Vision. Cambridge University Press, 2nd Edition, 2003, 655p. doi: 10.1017/CBO9780511811685
15. Hirschmueller, H. Stereo processing by semiglobal matching and mutual information. IEEE Transactions on pattern analysis and machine intelligence, 2008, Vol. 30, pp. 328–341. doi: 10.1109/TPAMI.2007.1166
16. Furukawa, Y., Ponce, J., 2010. Accurate, dense, and robust multi-view stereopsis. IEEE Transactions on Pattern Analysis and Machine Intelligence, 2010, Vol. 32, 1362–1376. doi: 10.1109/CVPR.2007.383246
17. Rothermel, M., Wenzel, K., Fritsch, D., and Haala, N. (2012). SURE: Photogrammetric surface reconstruction from imagery. In Proceedings of LowCost 3D Workshop Berlin, 2012, Vol. 2, pages 1–9.
18. Wenzel, K.; Abdel-Wahab, M.; Cefalu, A. & Fritsch, D. High-Resolution Surface Reconstruction from Imagery for Close Range Cultural Heritage Applications. The International Archives of the Photogrammetry, Remote Sensing and Spatial Information Sciences, 2012, Vol. XXXIX Part B5, p. 133-138, Commission V, XXIIth ISPRS Congress, Melbourne, Australia. doi: 10.5194/isprsarchives-XXXIX-B5-133-2012
19. Rothermel, M. Development of a SGM-Based Multi-View Reconstruction Framework for Aerial Imagery. Reihe C, Nr. 792, München 2016, ISBN 978-3-7696-5204-8, 115 S., (Softcopy only).
20. Wenzel, K. Dense Image Matching for Close Range Photogrammetry. Dissertation Universität Stuttgart, 2016. doi: 10.18419/opus-9027
21. Gong, K. & Fritsch, D. (2019). DSM generation from high resolution multi-view stereo satellite imagery. Photogrammetric Engineering & Remote Sensing, 2019, Vol. 85, pp. 379–387. doi: 10.14358/PERS.85.5.379
22. Facciolo, G., De Franchis, C., Meinhardt, E. MGM: A significantly more global matching for stereovision, in: Proceedings of BMVC 2015- 415 British Machine Vision Conference, 2015, pp. 1–12. doi: 10.5244/C.29.90
23. Besl, P.J & McKay, N.D. A method for registration of 3-D shapes. IEEE Transactions on Pattern Analysis and Machine Intelligence, 1992, Vol. 14, pp. 239-256. doi: 10.1109/34.121791.
24. Koch, K.R. Parameter Estimation and Hypothesis Testing in Linear Models. Springer, Berlin, 1999, 333p. doi: 10.1007/978-3-662-03976-2
25. Broelmann, J. Intuition und Wissenschaft in der Kreiseltechnik: 1750 bis 1930; Deutsches Museum: München, Germany, 2002.
26. Wagner, J.F.; Trierenberg, A. The Machine of Bohnenberger. In: *The History of Theoretical, Material and Computational Mechanics*; Stein, E., Ed.; Springer: Heidelberg, Germany, 2014, pp. 81-100. doi: 10.1007/978-3-642-39905-3_6
27. Wagner, J.F.; Perlmutter, M. The ISS Symposium Turns 50: Trends and Developments of Inertial Technology during Five Decades. Europ. J. Navig. 2015, Vol. *13*, No. 3, pp. 13-23. doi: 10.13140/RG.2.1.4396.8241
28. Magnus, K. *Kreisel: Theorie und Anwendungen*; Springer: Berlin, Germany, 1971. doi: 10.1007/978-3-642-52162-1
29. Shepp, L. A. &Vardi, Y. Maximum Likelihood Reconstruction for Emission Tomography." *IEEE Transactions on Medical Imaging* 1, 1982, No. 2, pp. 113-122. doi: 10.1109/TMI.1982.4307558

30. Remez, T., Litany, O., Giryes, R. & Bronstein, A.M. Deep Convolutional Denoising of Low-Light Images. In: CoRR abs/1701.01687. 2017. 11p., arXiv url: http://arxiv.org/abs/1701.01687.
31. Green, P.J. Bayesian Reconstructions from Emission Tomography Data using a modified EM Algorithm. In: IEEE Transactions on Medical Imaging, 1990, Vol. 9, No. 1, pp. 84-93. doi: 10.1109/42.52985.
32. Heinzl, C., Kastner, J., Gröller, E. Surface Extraction from Multi-Material Components for Metrology using Dual Energy CT," in IEEE Transactions on Visualization and Computer Graphics, vol. 13, no. 6, pp. 1520-1527, Nov.-Dec. 2007, doi: 10.1109/TVCG.2007.70598.
33. Lin, C. F., Yang, D. L., & Chung, Y. C. (2001, July). A marching voxels method for surface rendering of volume data. In *Proceedings. Computer Graphics International 2001*, pp. 306-313). IEEE.
34. https://www.volumegraphics.com/
35. Zhan, K., Fritsch, D. & Wagner, J.F. Stability Analysis of Intrinsic Camera Calibration Using Probability Distributions. Pres. Paper submitted to the 7th AMMSE 2020 Conference, Taipei, Taiwan, 2020 (in print).
36. Tang, R. Mathematical Methods for Camera Self-calibration in Photogrammetry and Computer Vision. Dissertation, University of Stuttgart, Deutsche Geod. Kommission, Series C, No. 703, Munich, 2013.
37. Zhan, K., Song, Y., Fritsch, D., Mammadov, G. & Wagner, J.F. Computed Tomography Colouring Based on Photogrammetric Images. Int. Arch. Photogramm. Remote Sens. Spatial Inf. Sci., XLIII-B2-2020, 2020, pp. 369-373, doi: 10.5194/isprs-archives-XLIII-B2-2020-369-2020
38. Bohnenberger, J.G.F. Beschreibung einer Maschine zur Erläuterung der Geseze der Umdrehung der Erde um ihre Axe, und der Veränderung der Lage lezteren. *Tübinger Blätter für Naturwissenschaften und Arzneikunde*, **1817**, *3*, pp. 72-83.
39. Tobin, W. The Life and Science of Léon Foucault. *Cambridge University Press: Cambridge, UK,* 2003.
40. Steinwand, J.-U. Der Fehler eines Kurskreisels beim Looping. Diplomarbeit (not published), TH Stuttgart, Stuttgart, 1966.
41. The Gyrolog Project, Oral History Interviews #1 with Joerg F. Wagner, #2 with Joerg Steinwand, and #3 with Helmut Sorg. Stuttgart, 2018.
42. Cohausz, P. W. *Cockpits deutscher Flugzeuge. Historische Instrumentierung von 1911-1970*. 1st ed.; Aviatic Verlag GmbH, Oberhaching, Germany, 2000; pp. 189, 190, 192, 217-227.
43. Schmid, W. Taumelfehler eines Kurskreisels. PhD Thesis, University of Stuttgart 1967, Stuttgart.
44. Siemens Archiv, Berlin. Documents with the signature: SAA 6994.
45. Unknown Authors, Fl.22561 Kurskreisel, 1944, https://www.deutscheluftwaffe.de/fl-22561-kurskreisel-1944 (accessed on 02.10.2020).
46. Heidler, M. Deutsche Fertigungskennzeichen bis 1945, Visier-Edition, Bad Ems, 2007. p. 176, 377.
47. Siemens Archiv, Berlin. Documents with the Signature: SAA 10790.; Klein, Gerald. *Dokumentation zur Geschichte des Luftfahrtgerätewerk Hakenfelde LGW 1930-1945*. 1st ed.; Werner-von-Siemens-Institut für Geschichte. Munich, Germany, 1980.; Kürvers, Klaus: Der "Hertlein-Bau" oder das ehemalige Luftfartgerätewerk (LGW) Hakenfelde. Berlin-Spandau, Streitstraße 5-22. (Architekt Hans Hertlein 1938-1942). Baugeschichtliche Dokumentation, Berlin, 2001, Part 1, 1-5. http://klausk.berlin/wp-content/uploads/2016/03/Hertleinbau-bauhist-Dok-InhaltTeil-1.pdf (accessed on 02.10.2020).
48. Etzkowitz, H.; Leydesdorff, L. (Eds.). Universities and the Global Knowledge Economy. A Triple Helix of University-Industry-Government Relations. Pinter, London, 1997.
49. Trischler, H. *The "Triple Helix" of Space. German Space Activities in a European Perspective.* Noordwijk: ESA, HSR-28, 2002. http://www.esa.int/esapub/hsr/HSR_28.pdf (accessed on 02.10.2020).
50. Archival sources from the Collection on Gyro Technology and Inertial Navigation, University of Stuttgart.
51. Unknown Authors. Starfighter – Ein gewisses Flattern. Der Spiegel. 1966, 5, pp. 21-36
52. Goobi: Das Community Portal für alle Themen rund um Goobi. Available online: https://goobi.io (accessed on 21/10/2020)
53. Deutsche Nationalbibliothek: The Integrated Authority File. Available online: https://www.dnb.de/EN/Professionell/Standardisierung/GND/gnd_node.html (accessed on 21/10/2020)
54. Ridge, M.: Crowdsourcing Our Cultural Heritage: Introduction. In: *Crowdsourcing Our Cultural Heritage*; Ridge, M., Ed.; Ashgate: Aldershot, UK, 2014, pp. 1–15.